2012

Discrete-Time Load Disturbance Torque Estimation for a DC Drive System

Huijie Qian
University of Windsor

Discrete-Time Load Disturbance Torque Estimation for a DC Drive System

by

Huijie Qian

A Thesis

Submitted to the Faculty of Graduate Studies

through the Department of Electrical and Computer Engineering

in Partial Fulfillment of the Requirements for

the Degree of Master of Applied Science at the

University of Windsor

Windsor, Ontario, Canada

2012

Discrete-Time Load Disturbance Torque Estimation for a DC Drive System

by

Huijie Qian

APPROVED BY:

_____

Dr. Bruce Minaker, Outside Departmental Reader

Department of Mechanical, Automotive and Materials Engineering

_____

Dr. Narayan Kar, Departmental Reader

Department of Electrical and Computer Engineering

_____

Dr. Xiang Chen, Advisor

Department of Electrical and Computer Engineering

_____

Dr. Chunhong Chen, Chair of Defense

Department of Electrical and Computer Engineering

May 10, 2012

DECLARATION OF CO-AUTHORSHIP / PREVIOUS PUBLICATION

I. Co-Authorship Declaration

I hereby declare that this thesis incorporates material that is result of joint research, as follows:

This thesis also incorporates the outcome of a joint research undertaken in collaboration with Danny Grignion under the supervision of professor Xiang Chen. The collaboration is covered in Chapters 2, 3 and 5 of the thesis. In all cases, the key ideas, primary contributions, experimental designs, data analysis and interpretation, were performed by the author, and the contribution of co-authors was primarily through the provision of revision of calculations and test setup.

I am aware of the University of Windsor Senate Policy on Authorship and I certify that I have properly acknowledged the contribution of other researchers to my thesis, and have obtained written permission from each of the co-author(s) to include the above material(s) in my thesis.

I certify that, with the above qualification, this thesis, and the research to which it refers, is the product of my own work.

II. Declaration of Previous Publication

This thesis includes one original paper that has been previously published/submitted for publication in peer reviewed journals, as follows:

Thesis Chapter	Publication title/full citation	Publication status
Chapter 2，3，5	Discrete Time Robust Load Disturbance Torque Estimator for a DC Motor Drive System	Submitted

I certify that I have obtained a written permission from the copyright owner(s) to include the above published material(s) in my thesis. I certify that the above material describes work completed during my registration as graduate student at the University of Windsor.

I declare that, to the best of my knowledge, my thesis does not infringe upon anyone's copyright nor violate any proprietary rights and that any ideas, techniques, quotations, or any other material from the work of other people included in my thesis, published or otherwise, are fully acknowledged in accordance with the standard referencing practices. Furthermore, to the extent that I have included copyrighted material that surpasses the bounds of fair dealing within the meaning of the Canada Copyright Act, I certify that I have obtained a written permission from the copyright owner(s) to include such material(s) in my thesis.

I declare that this is a true copy of my thesis, including any final revisions, as approved by my thesis committee and the Graduate Studies office, and that this thesis has not been submitted for a higher degree to any other University or Institution.

ABSTRACT

A DC motor is one of the most useful types of electrical motors and can be found in a variety of applications. However, it is well-known that there may exist a disturbance torque that acts on the motor shaft. Knowledge of that disturbance torque can be used to maintain good performance and stability. Unfortunately, direct measurement can be difficult and high in cost. In this case, an observer-based estimator can be designed to generate an estimate of the disturbance torque without the use of expensive sensors. A good estimator not only produces an appropriate estimate but also ensures that the estimate is insensitive to other factors such as noise or uncertainty. The estimator design is conducted in discrete time for direct implementation. All of the estimator designs are tested in a Hardware-in-loop (HIL) test bench under different load disturbance torque conditions and their performances are compared.

Key words: Discrete-Time, State Observer, Disturbance Torque Estimation

DEDICATION

My parents for their encouragement, support, and love.

ACKNOWLEDGEMENTS

I would like to sincerely thank my supervisor Dr. Xiang Chen for his guidance, instruction and encouragement during this research.

I would also like to thank Dr. Narayan Kar and Dr. Bruce Minaker for their inspiring suggestions and advice in this thesis and throughout this work.

I am deeply grateful to all my colleagues in the Advanced Control System Laboratory. I would especially like to thank my research partner, Danny Grignion, for his kind help and support and FangFang Lin for her friendship.

I am truly grateful to University of Windsor for their support during my graduate studies, along with the faculty and staff for their help and encouragement during these two years.

Finally, I am most grateful to my parents for their loving support.

TABLE OF CONTENTS

LIST OF TABLES

LIST OF FIGURES

ABBREVIATIONS

DC	Direct Current
DOB	Disturbance Observer
EMF	Electromotive Force
GUI	Graphic User Interface
HIL	Hardware-in-the-Loop
LAN	Local Area Network
PMDC	Permanent Magnet DC Motor
RC	Resistor-Capacitor
VDC	Voltage of Direct Current

NOMENCLATURE

Δ	Variation
τ_d	Disturbance Torque
ω_m	Motor Speed
B_m	Motor Viscous Friction Coefficient
G_a	Amplifier Gain
I_a	Armature Current
J_m	Motor Inertial Coefficient
K_t	Mechanical Constant
K_v	Electrical Constant
L_a	Armature Inductance
R_a	Armature Resistance
R_{shunt}	Current Shunt Resistance
T_{Load}	Load Torque Measurement
T_m	Mechanical Torque
V_b	Back emf Voltage
V_c	Analog Input Voltage
V_m	Terminal Voltage
V_o	Output Voltage of Amplifier
V_{out}	Output Voltage of Torque Sensor
V_t	Drive Voltage

CHAPTER 1

INTRODUCTION

It is generally known that a DC motor is one of the most useful types of electrical motors in the world. Its widespread use in a variety of fields results from some advantages over an AC motor. To begin with, a DC motor is designed to operate directly from a rechargeable battery, a solar cell or some other direct current power sources. In comparison with the control of an AC motor, speed control of a DC motor can be achieved much more easily. In addition, a DC motor is better suited for some precision motion control applications such as robots and disk drives. In the automotive sector, it is always used for valve control, window operation, and seat adjustment.

Since a real system is not ideal, it can be said that there always exists some inherent or external factors that affect the system process. For a DC motor, the disturbance torque acting on the shaft is one of the major factors. This disturbance torque can have an impact on the performance or the stability of a DC motor drive system. Thus, knowledge of the disturbance torque can provide a significant contribution to the design of a controller for a DC motor.

In the thesis, an observer-based disturbance torque estimator in discrete time is presented. By incorporating a state observer in the estimator, disturbance torque estimation can be achieved while also satisfying other performance or robustness requirements.

1.1 Disturbance Torque Estimation

As mentioned previously, the disturbance torque acting on the shaft will affect the system dynamics. Increasing or decreasing the disturbance torque will lead to a corresponding change of the armature current. A block diagram of a DC motor drive system is shown in Figure 1-1.

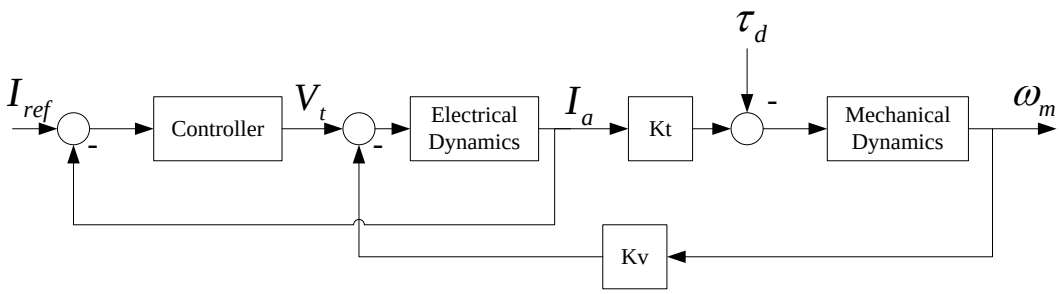

Figure 1-1 A DC Motor Drive System

It can be seen that the armature current is the controlled variable in the DC drive shown in Figure 1-1. For the purpose of maintaining a constant current as the reference, the knowledge of the disturbance torque is important and necessary. If the disturbance torque is estimated, the controller can take into account this variation and generate a corresponding control input to compensate for any changes. In comparison to the case where the disturbance torque is unavailable, the controller has a quicker reaction and better performance. As a result, the DC motor drive system can be designed to be robust to the variations in the load disturbance torque. However, direct measurement of the disturbance torque with a sensor is not feasible since it will increase the cost of the overall system. Hence, estimation is a feasible and effective means of use under these circumstances.

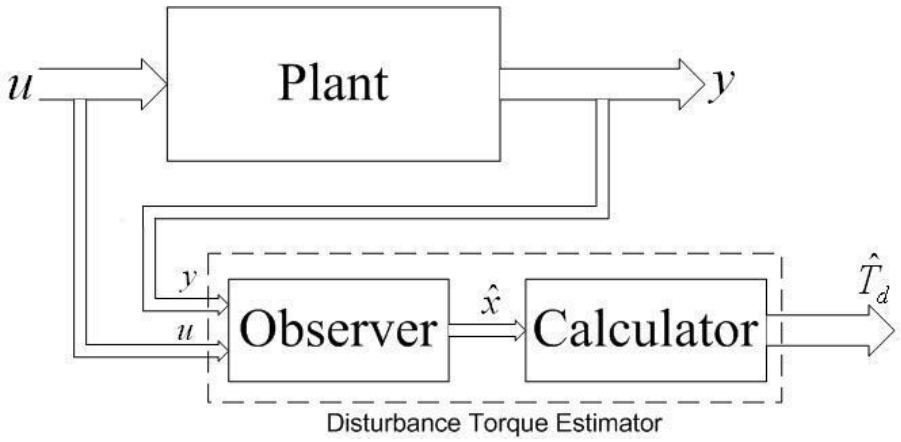

Figure 1- 2 A General Layout of the System with a Disturbance Torque Estimator

Figure 1-2 refers to a general layout of the system with a disturbance torque estimator. It is noted that the structure of the disturbance torque estimator is formed by a full-order state observer followed by a calculator. The state observer can deliver an appropriate estimation of the state variables of the plant model. Based on the estimated state variables, the disturbance torque estimation can be generated via a calculator.

In addition to the estimation of the disturbance torque, the estimator is capable of satisfying other requirements due to the incorporation of the state observer. Considering various optimization criteria in the state observer design, the overall estimator can be designed to realize desired performance or robustness requirements and generate an estimate simultaneously.

1.2 Design in Discrete-Time

It is well-known that most of the hardware controllers in use nowadays are digital devices. This leads to a significant advantage of design in discrete-time over design in continuous-time. By comparison, design in discrete-time provides a solution to the problem that can be directly implemented in modern digital controllers. This is a result of the fact that design in discrete time does not require discretization. This allows for the use of low-cost computers that reduce the overall cost of the system. Moreover, avoiding the degradation associated with discretizing a continuous-time design may result in an improvement in the system performance.

Although design in discrete-time may share some similarity with that in continuous-time, in some cases these two parallel developments still have a lot of differences. For example, only the plant model in discrete-time design needs to be discretized whereas the final observer design in continuous-time design needs to be discretized prior to implementation. Different solutions will also be presented for the design of the observer in the disturbance torque estimator.

1.3 Literature Review

By recognizing that a full-order steady-state observer is used in the estimator scheme, it can be stated that the observer design is of great importance. The state observer is designed to deliver estimates of state variables by means of an observer gain that is to be designed. Based on various criteria, a state observer can be designed to deal with the

effect of internal or external factors in a real physical system while also generating state estimations. In other words, the disturbance torque estimator that incorporates an observer contains an inherent freedom of design where some performance or robustness requirements can be satisfied.

In [1], three schemes for the design of a disturbance torque estimator for a DC drive are developed. In order to incorporate disturbance torque into the plant model, a solution is presented by extending the classical state observer. Two approaches are presented to realize that extension: one is to treat the disturbance torque as an unknown input and the other is to define it as a state variable. Regardless of which approach is used, they both assume that the disturbance torque is a constant or nearly constant value. In addition, the state observer constructed in the estimator scheme is a Luenberger observer, which is designed for a nominal plant model. As a result of these restrictions, this type of estimator is not applicable for implementation in a real physical system.

Taking into account that noise and uncertainty are unavoidable occurrences for a real physical system, the observer design should consider these effects within some optimization criteria. Over the past few years, many optimization criteria and methods have been proposed in literature. Solutions for both continuous-time systems and discrete-time systems have been developed.

In order to minimize the effect of undesirable white noise from the estimation, [2],[3] presents a Kalman filter design in discrete time. Two basic requirements are considered in the filter algorithm. One is to keep the expected value of the estimation equal to the

expected value of the state. Another is that the estimation varies from the state as little as possible. Based on those two design requirements, the overall filter design is formulated by three equations: a filter state equation, a discrete time Riccati equation (DARE), and a filter gain equation. It is noted that a recursive structure is applied to update the solution of the DARE every sampling period.

Apart from noise, model uncertainty is another common factor which affects the system process. Attenuation of model uncertainties receives much attention in observer design. One such a filter scheme is discussed in [4] and [5] known as the H_∞ filter. Instead of minimizing the variance of the estimation error, the H_∞ filter emphasizes the minimization of the worst case estimation error. The desired robustness to model uncertainty can be achieved by constraining the H_∞ norm of the transfer function from the uncertainty to the error in estimation. This can be done by using a filter gain that is calculated from the solution of a DARE. Some other designs for robust estimation are presented in [6], [7], and [8].

In some practical applications, the system is subjected to both white noises and model uncertainties. Thus a question arises as to how an estimator design could be conducted to satisfy noise rejection and uncertainty attenuation. In this case, a H_∞ Gaussian filter is designed in [9] via a game theory methodology. By introducing a selection parameter γ, the filter can achieve optimal state estimation that balances noise rejection and uncertainty attenuation. Other methods and approaches are also proposed in [10], [11], and [12] to solve this multi-objective problem.

Although the filter design introduced previously can deal with white noises, model uncertainties or both, none of them places emphasis on delivering the most accurate estimation of the disturbance torque. Using the H_∞ filter as an example, the algorithm aims to minimize (constrain) the sensitivity of the estimation error to model uncertainties while ignoring the sensitivity to the disturbance torque. As a result, accurate estimation is not guaranteed since the algorithm only places focus on suppressing model uncertainties. In order to accomplish this task, a combined multi-objective filter design is conducted in [13]. A new measurement called the H_ index is utilized for the purpose of maximizing the sensitivity of a signal. Some other examples of similar design are presented in [14], [15], and [16].

1.4 Research Objective

The main goal of this thesis is to design a disturbance torque estimator in discrete time. The overall estimator design consists of a discrete-time state observer and a discrete-time disturbance torque calculator.

The following discrete-time state observers are discussed in the thesis:

(1) Luenberger observer

(2) Kalman observer

(3) H_∞ observer

(4) Mixed H_2/H_∞ observer

(5) H_ / H_∞ observer

1.5 Thesis Outline

The thesis is organized as follows:

Chapter 2 provides a theoretical background of a general observer design in discrete time. Different algorithms or criteria utilized for the observer design are introduced in detail.

Chapter 3 discusses the design of a general disturbance torque estimator for a DC motor drive system in discrete time. Applications of different observer designs into the estimation scheme are detailed as well.

Chapter 4 presents a configuration of the Hardware-in-the-loop testbench used to test the estimator designs which includes the configurations of major physical components and the software used for real-time simulation.

Chapter 5 shows the test results of the disturbance torque estimator with the use of the HIL testbench. Based on the different observers incorporated into the estimator, the test results are analyzed.

Chapter 6 concludes this thesis. Some ideas about the improvement of the estimator designs and future work are presented.

CHAPTER 2

THEORETICAL BACKGROUND

2.1 Definitions of Norms

Prior to the observer design in discrete-time, some definitions associated with the criteria or algorithm of the observer will be introduced first. In [4], [5], [13], and [14], the H_2 norm, the H_∞ norm, and the H_ index will be defined as follows:

For a discrete-time transfer matrix $G(z) \in \mathcal{RH}_2$, the H_2 norm can be defined as

$$\|G\|_2 = \sqrt{\frac{1}{2\pi}\int_0^{2\pi} \text{Trace}[G^{\sim}(e^{J\theta})G(e^{J\theta})]\, d\theta}.$$

where $\mathcal{RH}_2$ is the space of all strictly proper and real rational matrix transfer functions

For $G(z) \in \mathcal{RH}_\infty$, the H_∞ norm can be defined as

$$\|G\|_\infty = \sup_{\theta\in[0,2\pi]} \overline{\sigma}\left[G(e^{J\theta})\right].$$

where $\mathcal{RH}_\infty$ is the space of all proper and real rational matrix transfer functions

The H_ index of *G* on the whole unit circle can be defined as

$$\|G\|_{\_}^{[0,2\pi]} = \inf_{\theta\in[0,2\pi]} \underline{\sigma}\left[G(e^{J\theta})\right].$$

The H_ index of *G* over a finite frequency range $[\theta_1, \theta_2]$ can be defined as

$$\|G\|_{\_}^{[\theta_1,\theta_2]} = \inf_{\theta\in[\theta_1,\theta_2]} \underline{\sigma}\left[G(e^{J\theta})\right]$$

The H_ index of *G* at zero frequency ($\theta = 0$) can be defined as

$$\|G\|_{\_}^{[0]} = \underline{\sigma}[G(1)]$$

2.2 Observer Design in Discrete-Time

Observers are desirable in many situations in engineering. As mentioned previously, state variables of a system are not necessarily available. Hence, a state observer provides a feasible approach to estimate or observe these state variables. In addition to achieving estimation, a good algorithm of a state observer can help to avoid the degradation of the estimation of the state variables in a real practical system.

Consider a state space model in continuous time

$$\dot{x}(t) = Ax(t) + Bu(t) \qquad (2\text{-}1)$$
$$y(t) = Cx(t)$$

Since all the designs are conducted in discrete-time, a discrete-time representation of the state space model can be given as

$$x(k+1) = G(T)x(k) + H(T)u(k) \qquad (2\text{-}2)$$
$$y(k) = Cx(k)$$

where $G(T) = e^{AT}, \ H(T) = (\int_0^T e^{A\lambda} d\lambda)B$

It is noted that $G(T)$, $H(T)$ are matrices that depend on the sampling period T. With a fixed sampling period T, the state space model of a system in discrete time can be represented as

$$x(k+1) = Gx(k) + Hu(k) \qquad (2\text{-}3)$$
$$y(k) = Cx(k)$$

For any linear, time-invariant, discrete-time, system, a general observer model [17] can be

developed with the assumption that the pair (G, C) is observable:

$$\hat{x}(k+1) = G\hat{x}(k) + Hu(k) + L[y(k) - \hat{y}(k)] \quad (2\text{-}4)$$

$$\hat{y}(k) = C\hat{x}(k)$$

where L is the observer gain matrix. A system with a state observer in discrete-time is shown in Figure 2-1.

It can be seen in Figure 2-1 that there exists a correction term $L[y(k) - \hat{y}(k)]$ in the observer structure. This additional term plays a significant role in the observer dynamics since the difference between the measurement output and estimation output with the observer gain can help to improve the performance of the observer.

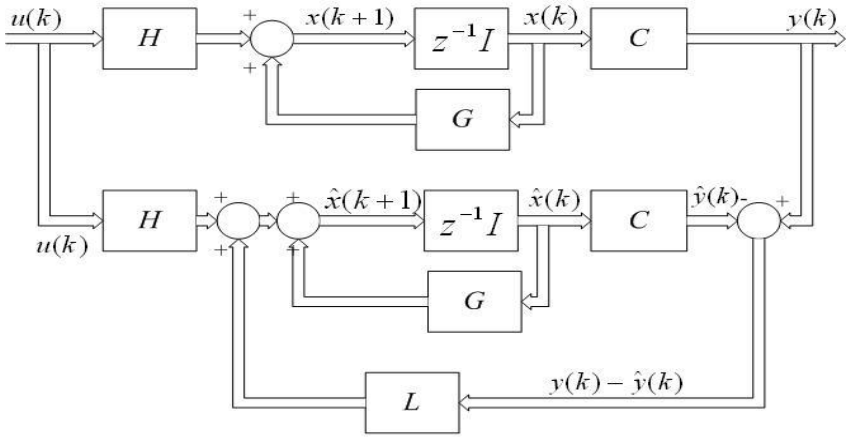

Figure 2- 1 System with a State Observer in Discrete-Time

2.3 Luenberger Observer

The Luenberger observer[18], [19] is the most basic and simplest observer design due to the assumption that there are no internal or external factors affecting the system. Thus, the

behavior of the Luenberger observer depends solely on the nominal plant model. The objective of the Luenberger observer is to make the behavior of the error in estimation faster than the behavior of the system response. The pole-placement[17] approach gives a solution to achieve this goal.

The error in estimation is defined as the difference between real state $x(k)$ and estimated state $\hat{x}(k)$

$$e(k) = x(k) - \hat{x}(k)$$

The error dynamics can be obtained by subtracting the state equation of the observer model from the system model

$$e(k+1) = x(k+1) - \hat{x}(k+1) \qquad (2\text{-}5)$$

$$= Gx(k) + Hu(k) - G\hat{x}(k) - Hu(k) - L[y(k) - \hat{y}(k)]$$

$$= G[x(k) - \hat{x}(k)] - L[Cx(k) - C\hat{x}(k)]$$

$$= (G - LC)[x(k) - \hat{x}(k)]$$

$$= (G - LC)e(k)$$

It can be noted in Equation 2-5 that the behavior of the error dynamics is determined by the eigenvalues of the matrix (G-LC) which can be treated as the poles of the observer. Then faster error dynamic behavior can be achieved by placing the poles of the observer in some desirable location within the unit circle. When the desirable observer poles are selected, a corresponding observer gain can be determined from the characteristic equation of the error dynamics equations. With the use of that appropriate observer gain L, the estimated state $\hat{x}(k)$ will converge to the real state $x(k)$ in an adequately quick speed and thus fast error dynamics can be achieved.

2.4 Kalman Observer

It is generally known that useful information is always affected by white noise in a real physical system. In this case, the Kalman observer[2],[20] is one of the most well-known filter to solve this problem. The algorithm of the observer is designed to minimize the effect of white noise appearing in the process or measurement branch and retain the useful information.

Consider a liner discrete-time system given as follows

$$x(k+1) = Gx(k) + Hu(k) + w(k) \quad (2\text{-}6)$$

$$y(k) = Cx(k) + v(k)$$

where $w(k)$, $v(k)$ denotes process noise and measurement noise, respectively. It is assumed that these white noises are zero-mean, uncorrelated and have known covariance.

The criteria of the Kalman observer is to minimize the H_2 norm[20] of the expected value of the estimation error, which can be formulated as a cost function $J = E[e^T(k)e(k)]$, where $E[]$ means the expected value.

The cost function J_k can be minimized by means of a steady-state observer gain matrix L_{KD}

$$L_{KD} = GPC^T(CPC^T + R)^{-1} \quad (2\text{-}7)$$

where P is the covariance of the estimation error, which can be calculated from a steady-state discrete-time algebraic Riccati equation(DARE)

$$P = GPG^T - GPC^T[(CPC^T + R)^{-1}]CPG^T + Q \quad (2\text{-}8)$$

and Q, R are known matrices that represent the covariance of process noise and measurement noise, respectively.

2.5 H_∞ Observer

In industrial problems, accurate system models are not always available due to the existence of some uncertainties. Under this circumstance, a robust observer that can tolerate model uncertainties gains much attention. An H_∞ observer [7],[20] is designed specifically to solve this robustness problem.

The state space model of the system can be given as

$$x(k+1) = Gx(k) + Hu(k) + w(k) \quad (2\text{-}9)$$

$$y(k) = Cx(k) + v(k)$$

$$z(k) = C_1 x(k)$$

where $w(k)$, $v(k)$ are the uncertainty terms and $z(k)$ is the signal to be estimated.

In contrast to the criteria of the Kalman observer that the expected value of the covariance of the estimation error is minimized, the H_∞ observer places focus on minimization of the worst-case estimation error. The objective of an H_∞ observer is to estimate $z(k)$ and minimize the following cost function J_∞. However, direct minimization is very difficult to realize, so instead a performance upper-bound γ is chosen such that the cost function can satisfy the following inequality

$$J_\infty = \lim_{N\to\infty} \frac{\sum_{k=0}^{N-1} \|z(k) - \hat{z}(k)\|_2^2}{\sum_{k=0}^{N-1} (\|w(k)\|_2^2 + \|v(k)\|_2^2)} \leq \gamma^2 \quad (2\text{-}10)$$

This can be done by solving the following steady-state discrete algebraic Riccati equation (DARE)

$$P = GPG^T - GP[(C^T R^{-1} C - \gamma^{-2} S)^{-1} + P]^{-1} PG^T + Q \quad (2\text{-}11)$$

where P is the stabilizing solution to the DARE, and R, S, Q are symmetric, positive-definite matrices chosen as a design parameter.

The observer gain matrix L_{HID} can be calculated using the following formula

$$L_{HID} = P[I - \gamma^{-2} SP + C^T R^{-1} C]^{-1} C^T R^{-1} \quad (2\text{-}12)$$

2.6 Mixed H_2/H_∞ Observer

There is a possibility that the system is subjected to both white noise and model uncertainty. However, the Kalman observer is designed specifically to cope with a stochastic signal with known power spectral density while the H_∞ observer is only designed to solve the robustness problems. Thus, an observer that can satisfy these two requirements is hence of great interest. A mixed H_2/H_∞ observer[9],[10] in discrete time derived from the Nash game is proposed to resolve this problem. The algorithm of the observer considers a constrained optimization problem formulated by two coupled discrete algebraic Riccati equation (DARE). A steady-state filter gain matrix can be given based on the solution to these two DARE.

The state space model of the system can be written as:

$$x(k+1) = Gx(k) + Hu(k) + H_0(k)w_0(k) + H_1(k)w(k) \quad (2\text{-}13)$$

$$y(k) = Cx(k) + D_{20}w_0(k)$$
$$z(k) = C_1x(k)$$

$$z_0(k) = C_0x(k)$$

Based on the general structure of an observer design, a mixed H_2/H_∞ observer is described as:

$$\hat{x}(k+1) = G\hat{x}(k) + Hu(k) + L_{MD}[y(k) - C_2\hat{x}(k)] \quad (2\text{-}14)$$

$$\hat{z}(k) = C_1\hat{x}(k)$$

$$\hat{z}_0(k) = C_0\hat{x}(k)$$

The steady-state observer gain matrix L_{MD} is designed to guarantee that the error $e(k) = z(k) - \hat{z}(k)$ and $e_0(k) = z_0(k) - \hat{z}_0(k)$ is minimized, respectively.

Prior to formulating the discrete-time mixed H_2/H_∞ observer problem, two cost functions considering H_∞ optimization and H_2 optimization are defined as:

$$J_1(F, w, w_0) = \gamma^2\|w\|_P^2 - \|e\|_P^2 \quad (2\text{-}15)$$

$$J_2(F, w, w_0) = \|e_0\|_P^2$$

where F represents an admissible observer: $\begin{bmatrix} y(k) \\ u(k) \end{bmatrix} \rightarrow \begin{bmatrix} \hat{z}(k) \\ \hat{z}_0(k) \end{bmatrix}$

Then a discrete-time mixed H_2/H_∞ observer problem can be formulated as the following two inequalities[10] :

$$J_1(F_*, w_*, w_0) \leq J_1(F_*, w, w_0) \quad (2\text{-}16)$$

$$J_2(F_*, w_*, w_0) \leq J_1(F, w_*, w_0)$$

The objective of a discrete-time mixed H_2/H_∞ observer is to design an admissible *F* in the form of Equation 2-14 such that the two inequalities are satisfied. Two coupled discrete algebraic Riccati equations are developed to characterize the problem:

$$P_1 = \bar{G}^T P_1 \bar{G} + \gamma^{-2} \bar{G}^T P_1 H_1 (I - \gamma^{-2} H_1^T P_1 H_1)^{-1} H_1^T P_1 \bar{G} + C_1^T C_1 \quad (2\text{-}17)$$

$$P_2 = G_F P_2 G_F^T - (H_0 D_{20}^T + G_F P_2 C_2^T)(R_0 + C_2 P_2 C_2^T)^{-1}(H_0 D_{20}^T + G_F P_2 C_2^T)^T + H_0 H_0^T$$

where $$I - \gamma^{-2} H_1^T P_1 H_1 > 0, \quad R_0 + C_2 P_2 C_2^T > 0$$

$$\bar{G} = G + L_* C_2, \quad \Delta_1 = I - \gamma^{-2} H_1 H_1^T P_1$$

$$G_F = (I + \gamma^{-2} H_1 H_1^T P_1 \Delta_1^{-1}) G + \gamma^{-2} H_1 H_1^T P_1 \Delta_1^{-1} L_* C_2$$

If there exist stabilizing solutions $P_1 \geq 0$ and $P_2 \geq 0$, an observer gain matrix L_{MD} can be obtained as:

$$L_{MD} = (G_F P_2 C_2^T + H_0 D_{20}^T)(R_0 + C_2 P_2 C_2^T)^{-1} \quad (2\text{-}18)$$

By using the observer gain matrix L_{MD}, the mixed H_2/H_∞ observer can find a trade-off between noise rejection and uncertainty attenuation.

2.7 H_/H$_\infty$ Observer

Apart from removing the effect of some undesirable factors, there should be a treatment of the signal that we place focus on. Thus a question arises that if a multi-objective criteria can be developed to maximize the sensitivity to the signal to be estimated and constrain the sensitivity to the undesirable signal. In this case, a multi-objective H_/H_∞ observer[14], [16] is conducted to accomplish this target.

The state space model used for the observer design can be written as:

$$x(k+1) = Gx(k) + Hu(k) + H_d(k)d(k) + +H_f(k)f(k) \qquad (2\text{-}19)$$
$$y(k) = Cx(k) + D_d d(k) + D_f f(k)$$

where $d(k)$ and $f(k)$ represents the disturbance signal and fault signal, respectively. Depending on the specific situation, they can be modeled as different types of signals.

By taking the ***z*** transform of Equation 2-19, we get the following input/output equation of the system

$$y(k) = G_u u(k) + G_d d(k) + G_f f(k) \qquad (2\text{-}20)$$

where G_u, G_d, G_f are transfer matrices and their state space realizations are

$$\begin{bmatrix} G_u & G_d & G_f \end{bmatrix} = \left[\begin{array}{c|ccc} G & H & H_d & H_f \\ \hline C & D & D_d & D_f \end{array}\right] \qquad (2\text{-}21)$$

Since G_u, G_d, G_f share the same *G* and *C*, a left coprime factorization[4] can be given

$$[G_u, G_d, G_f] = M^{-1}[N_u, N_d, N_f] \qquad (2\text{-}22)$$

where $[M, N_u, N_d, N_f] = \left[\begin{array}{c|ccc} G+LC & L & H+LD & H_d+LD_d & H_f+LD_f \\ \hline C & I & D & D_d & D_f \end{array}\right]$

and *L* is a gain matrix such that *G+LC* is stable.

Without loss of generality, the following structure is used for the observer design:

$$r = Q(My - N_u u) = Q\left[M\left(G_u u + G_d d + G_f f\right) - N_u u\right] \qquad (2\text{-}23)$$
$$= Q\left[M\left(M^{-1}N_u u + M^{-1}N_d d + M^{-1}N_f f\right) - N_u u\right]$$
$$= QN_d d + QN_f f = G_{rd} d + G_{rf} f$$

Where r is a residual vector for detection and Q is a free stable matrix to be designed. Then, a multi-objective criteria can be defined as to design a Q such that G_{rd} is constrained by a rejection level γ and $\|G_{rf}\|_-$ is maximized, i.e.[14]

$$\max_{Q\in\mathcal{RH}_\infty} \left\{ \|QN_f\|_- : \ \|QN_d\|_\infty \le \gamma \right\} \tag{2-24}$$

Prior to the design of an appropriate Q, a matrix V can be defined as

$$V = \left[\begin{array}{c|c} G+L_0C & [(G+L_0C)PC^T+(H_d+L_0D_d)D_d^T]R_d^{-1/2} \\ \hline C & R_d^{1/2} \end{array}\right] \tag{2-25}$$

where $R_d = CPC^T + D_dD_d^T$, $L_0 = -(GPC^T + H_dD_d^T){R_d}^{-1}$ and P can be solved using the following discrete algebraic Riccati equation (DARE).

$$P = GPG^T - (GPC^T + H_dD_d^T){R_d}^{-1}(D_dH_d^T + CPG^T) + H_dH_d^T \tag{2-26}$$

Using the inequality $\|AB\|_- \le \|A\|_\infty \|B\|_-$, the multi-objective criteria in Equation 2-24 can be rewritten as

$$\|QN_f\|_- = \|QVV^{-1}N_f\|_- \le \|QV\|_\infty \|V^{-1}N_f\|_- \tag{2-27}$$
$$\|QN_f\|_- \le \|QN_d\|_\infty \|V^{-1}N_f\|_- \le \gamma \|V^{-1}N_f\|_-$$

Thus,

$$\max\left\{ \|G_{rf}\|_- : \ \|G_{rd}\|_\infty \le \gamma \right\} = \max\left\{ \|QN_f\|_- : \ \|QN_d\|_\infty \le \gamma \right\} = \gamma \|V^{-1}N_f\|_- \tag{2-28}$$

and a multi-objective observer can be carried out in the following form

$$r = Q_{opt}\,[M \quad -N_u]\begin{bmatrix} y \\ u \end{bmatrix} = \gamma V^{-1}[M \quad -N_u]\begin{bmatrix} y \\ u \end{bmatrix} = \tag{2-29}$$

$$\gamma\left[\begin{array}{c|cc} G + L_0 C & -L_0 & B + L_0 D \\ \hline -R_d^{-1/2} C & R_d^{-1/2} & -R_d^{-1/2} D \end{array}\right]$$

In other words, an H_/H$_\infty$ observer can be developed as

$$\hat{x}(k+1) = G\hat{x}(k) + Hu(k) + L_0[C\hat{x}(k) - y(k)] \tag{2-30}$$

$$r(k) = \gamma[R_d{}^{-\frac{1}{2}}(y(k) - \hat{y}(k))]$$

CHAPTER 3

DISCRETE-TIME DISTURBANCE TORQUE ESTIMATOR DESIGN

3.1 State Space Model of a DC Motor in Discrete-Time

In the thesis, the disturbance torque estimator is applied to a DC motor drive system. Figure 3-1 illustrates an electro-mechanical model of a DC motor.

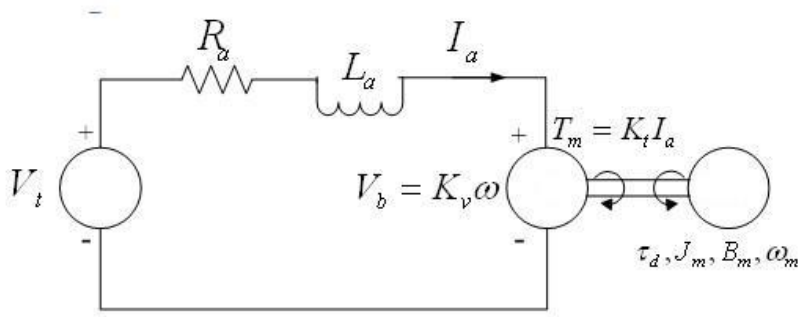

Figure 3- 1 DC Motor Model

It can be seen that the electric circuit of a DC motor consists of the drive voltage V_t, the armature resistance R_a, the armature inductance L_a, and the back emf voltage V_b. Due to the fixed field in a PMDC, the electrical dynamics can be represented as

$$V_t = R_a I_a + L_a \frac{dI_a}{dt} + V_b \quad (3\text{-}1)$$

where $V_b = K_v \omega_m$ and opposes the drive voltage V_t[21], By substituting the back emf voltage with its representation of motor speed, the electrical equation of a DC motor

model can be formulated as

$$V_t = R_a I_a + L_a \frac{dI_a}{dt} + K_v \omega \tag{3-2}$$

Since a DC motor is an electro-mechanical device, the modeling of the mechanical behavior is also important. By using Newton's laws, the mechanical equation of a DC motor can be written as

$$K_t I_a = J_m \frac{d\omega_m}{dt} + B_m \omega_m + \tau_d \tag{3-3}$$

Note that $K_t I_a$ stands for a mechanical torque generated by the motor.

Based on Equation 3-2 and Equation 3-3, the state space model of a DC motor can be written as

$$\dot{x}(t) = Ax(t) + Bu(t) \tag{3-4}$$

$$y(t) = Cx(t)$$

where

$$x = \begin{bmatrix} I_a \\ \omega_m \end{bmatrix}, \quad u = V_t, \quad y = I_a$$

$$A = \begin{bmatrix} -\frac{R_a}{L_a} & -\frac{K_v}{L_a} \\ \frac{K_t}{J_m} & -\frac{B_m}{J_m} \end{bmatrix}, \qquad B = \begin{bmatrix} \frac{1}{L_a} \\ 0 \end{bmatrix}, \qquad C = [1 \quad 0]$$

It is noted that the state space model is a nominal plant model, which does not include the load disturbance torque τ_d or any other factors. Those factors will be incorporated into the system model in order to satisfy the specific requirements of the observer design. The armature current is defined as the only measurement output of the system due to the high cost of an encoder for speed measurement.

For the purpose of facilitating the design in discrete time, it is necessary to discretize the state model. Using a sampling period *T*, the state space model can be rewritten as

$$x(k+1) = Gx(k) + Hu(k) \qquad (3\text{-}5)$$

$$y(k) = Cx(k)$$

where $G = e^{AT}$, $H = \left(\int_0^T e^{A\lambda} d\lambda\right) B = (e^{AT} - I)A^{-1}B$

Since the DC motor model will be used for the state observer design, the observability of the plant should be considered first. As mentioned previously, the system is completely observable if the following matrix has full column rank.

$$\begin{bmatrix} C \\ CG \end{bmatrix} = \begin{bmatrix} 1 & 0 \\ G_{11} & G_{12} \end{bmatrix} \qquad (3\text{-}6)$$

where G_{11}, G_{12} are the elements in the first row in matrix *G*.

It can be seen clearly in Equation 3-6 that the observability matrix has the full column rank. Hence, the state variables of the DC motor $x(k)$ can be obtained from its input $u(k)$ and output $y(k)$.

3.2 Design of a General Disturbance Torque Calculator in Discrete-Time

For the purpose of incorporating the observer design into the disturbance torque estimator, a calculator that relates the disturbance torque estimation to the estimation of the state variables and their derivatives is required.

In continuous time, the following equation is derived to estimate the disturbance torque

according to the mechanical behavior of a DC motor.

$$\hat{\tau}_d(t) = K_t I_a(t) - J_m \dot{\hat{\omega}}_m(t) - B_m \hat{\omega}_m(t) \tag{3-7}$$

Comparing to the mechanical equation in Equation 3-3, ω_m and $\dot{\omega}_m$ are replaced with their estimations. However, $I_a(t)$ is still used here instead of $\hat{I}_a(t)$ since it is assumed that the measurement is more reliable than the estimation.

In order to discretize this estimation, the equation is reorganized as follows

$$\begin{aligned} \dot{\hat{\omega}}_m(t) &= -\frac{B_m}{J_m}\hat{\omega}_m(t) + \frac{K_t}{J_m} I_a(t) - \frac{1}{J_m}\hat{\tau}_d(t) \\ &= -\frac{B_m}{J_m}\hat{\omega}_m(t) + \begin{bmatrix} \frac{K_t}{J_m} & -\frac{1}{J_m} \end{bmatrix} \cdot \begin{bmatrix} I_a(t) \\ \hat{\tau}_d(t) \end{bmatrix} \end{aligned} \tag{3-8}$$

With the use of a sampling period *T*, the equation above can be discretized in the following form

$$\begin{aligned} \hat{\omega}(k+1) = e^{-\frac{B_m}{J_m}\cdot T}\hat{\omega}(k) + \left(e^{-\frac{B_m}{J_m}\cdot T} - 1\right) \cdot \left(-\frac{B_m}{J_m}\right)^{-1} \\ \cdot \begin{bmatrix} \frac{K_t}{J_m} & -\frac{1}{J_m} \end{bmatrix} \cdot \begin{bmatrix} I_a(k) \\ \hat{\tau}_d(k) \end{bmatrix} \end{aligned} \tag{3-9}$$

Thus the disturbance torque estimate in discrete time can be written as

$$\hat{\tau}_d(k) = K_1 I_a(k) + K_2 \hat{\omega}(k) + K_3 \hat{\omega}(k+1) \tag{3-10}$$

where $K_1 = -\dfrac{K_t\left(e^{-\frac{B_m}{J_m}\cdot T} - 1\right)\cdot\left(-\frac{B_m}{J_m}\right)^{-1}/J_m}{\left(e^{-\frac{B_m}{J_m}\cdot T} - 1\right)\cdot\left(-\frac{B_m}{J_m}\right)^{-1}/J_m} = K_t,\ K_2 = -\dfrac{e^{-\frac{B_m}{J_m}\cdot T}}{\left(e^{-\frac{B_m}{J_m}\cdot T} - 1\right)\cdot\left(-\frac{B_m}{J_m}\right)^{-1}/J_m}$

and $K_3 = \frac{1}{\left(e^{-\frac{B_m}{J_m}\cdot T} - 1\right)\cdot(-\frac{B_m}{J_m})^{-1}/J_m}$

It can be seen in Equation 3-10 that the disturbance torque estimation is related to the estimation of the state variables and their derivatives in discrete time. A block diagram of the overall estimator is shown in Figure 3-2.

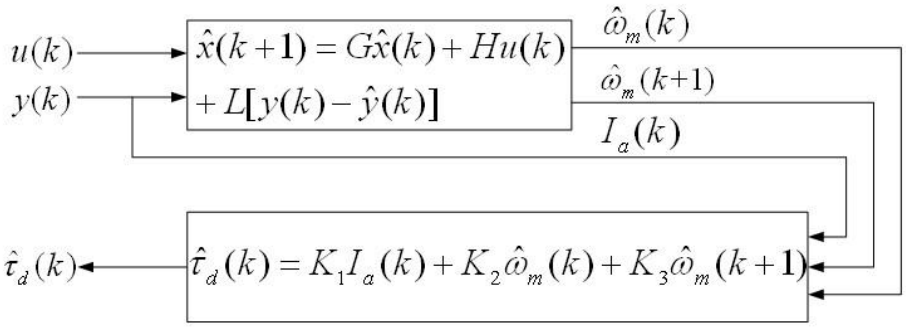

Figure 3- 2 Overall Disturbance Torque Estimator in Discrete-Time

With the finding that the disturbance torque estimation is obtained from the estimation of the state variables and their derivatives, there may exist an alternative simplification of the estimator.

By applying the system model of a DC motor into the general observer structure of Equation 2-4, the observer model can be written as

$$\begin{bmatrix} \hat{I}_a(k+1) \\ \hat{\omega}_m(k+1) \end{bmatrix} = e^{AT} \begin{bmatrix} \hat{I}_a(k) \\ \hat{\omega}_m(k) \end{bmatrix} + (e^{AT} - I)A^{-1}Bu(k) + \begin{bmatrix} L_1 \\ L_2 \end{bmatrix} e_i(k) \qquad (3\text{-}11)$$

where $e_i(k) = I_a(k) - \hat{I}_a(k)$ is the error in estimation of the armature current.

In order for the simplification to be achieved, some approximations need to be made. In

particular, we write

$$e^{AT} \approx AT + I, \qquad (e^{AT} - I)A^{-1}B \approx BT$$

Then, (3-11) can be reduced to the following:

$$\begin{bmatrix} \hat{I}_a(k+1) \\ \hat{\omega}_m(k+1) \end{bmatrix} = \begin{bmatrix} -\frac{R_a}{L_a} \cdot T + 1 & -\frac{K_v}{L_a} \cdot T \\ \frac{K_t}{J_m} & -\frac{B_m}{J_m} \cdot T + 1 \end{bmatrix} \cdot \begin{bmatrix} \hat{I}_a(k) \\ \hat{\omega}_m(k) \end{bmatrix} + \begin{bmatrix} L_1 \\ L_2 \end{bmatrix} e_i(k) \tag{3-12}$$

By noting that

$$\hat{\omega}_m(k+1) = \frac{K_t T}{J_m} \hat{I}_a(k) + (1 - \frac{B_m}{J_m} \cdot T)\hat{\omega}_m(k) + L_2 e_i(k) \tag{3-13}$$

and substituting Equation 3-13 into Equation 3-10, the equation of the disturbance torque estimation in discrete time becomes

$$\hat{\tau}_d(k) = \left(K_t - \frac{L_2 J_m}{T}\right) e_i(k) \tag{3-14}$$

It is noted that the disturbance torque estimation is now related to the error in armature current estimation, which yields a simplified approach to generate the estimation of the disturbance torque.

3.3 Observer Design

All the state observers introduced previously are used in the overall estimator scheme for the purpose of estimating the disturbance torque applied to a DC motor drive system. Depending on the observer used, different signals are included into the system model of the DC motor to satisfy the specific requirements of the observer performance. As

mentioned previously, the estimated disturbance torque can be obtained from the error in estimation. Thus, the performance of all the estimators will be discussed in terms of the analysis of error dynamics.

3.3.1 Luenberger Observer

Due to the assumption that the Luenberger observer design is based on a nominal plant model, the system model used for the observer design only considers the disturbance torque. For the Luenberger observer, the state space model of the DC motor can be given as

$$x(k+1) = Gx(k) + Hu(k) + H_d d(k) \qquad (3\text{-}15)$$

$$y(k) = Cx(k)$$

where $G,\ H,\ C,\ x(k),\ u(k),\ y(k)$ are defined as in Equation 3-4 and Equation 3-5,

and $H_d = \begin{bmatrix} 0 \\ -\frac{T}{J_m} \end{bmatrix},\ d(k) = \tau_d(k)$

The error dynamics of the disturbance torque estimator using a Luenberger observer can be written as:

$$e(k+1) = x(k+1) - \hat{x}(k+1) = (G - LC)e(k) + H_d\tau_d(k) \qquad (3\text{-}16)$$

The solution of the difference equation above is

$$e(k) = (G - L_{XD}\,C)^k e(0) + \sum_{n=0}^{k-1} (G - L_{XD}\,C)^n H_d \tau_d(k-n-1) \qquad (3\text{-}17)$$

Equation 3-17 shows the relationship between the disturbance torque and the estimation

error. It is noted that the estimator using a steady-state Luenberger observer is capable of delivering an estimation of a constant or a low-frequency disturbance (slower than the error dynamics). A steady state observer gain L_{XD} can be calculated using pole-placement method according to the following steps:

(1) Verify that the system is observable.

$$\text{rank}\left[C^T \;\vdots\; G^T C^T \;\vdots\; (G^T)^2 C^T \;\vdots\; \cdots \;\vdots\; (G^T)^{n-1} C^T\right] = n \tag{3-18}$$

(2) Calculate the poles of the system via the following characteristic equation.

$$|zI - G| = 0$$

(3) Place the poles of the observer by means of the following characteristic equation of the observer

$$|zI - (G - L_{XD} C_2)| = |zI - G + L_{XD} C_2| = 0 \tag{3-19}$$

By choosing the desired poles of the observer such that the error of the estimation converges to zero faster than the system poles, the steady-state observer gain matrix L_{XD} can be obtained.

It can be seen in Equation 3-16 that the error dynamics are derived from a nominal plant model. As a result of this restriction, the estimator design using a Luenberger observer is not desirable in practical applications.

3.3.2 Kalman Observer

In order to apply the Kalman observer into the disturbance torque estimator appropriately,

the system model of the DC motor is augmented with both white noises and the disturbance torque. It is general known that there always exists a variation in the brush voltage for a DC motor. In addition, white noise also appears in the measurement branch, where the current shunt resistor is used. Hence, a single vector $w_0(k)$ is introduced here to represent both process and measurement noises. A system with disturbance torque estimator using a Kalman observer is shown in Figure 3-3.

The state space model of the DC motor used for a Kalman observer can be written as:

$$x(k+1) = Gx(k) + Hu(k) + H_0 w_0(k) + H_d d(k) \qquad (3\text{-}20)$$
$$y(k) = Cx(k) + D_{20} w_0(k)$$

where $w_0(k) = \begin{bmatrix} V_{brus\,h}(k) \\ \Delta I_a(k) \end{bmatrix}, H_d = \begin{bmatrix} 0 \\ -\frac{T}{J_m} \end{bmatrix}$, $d(k) = \tau_d(k)$, and H_0, and D_{20} are matrices determined by covariances *Q* and *R*, respectively.

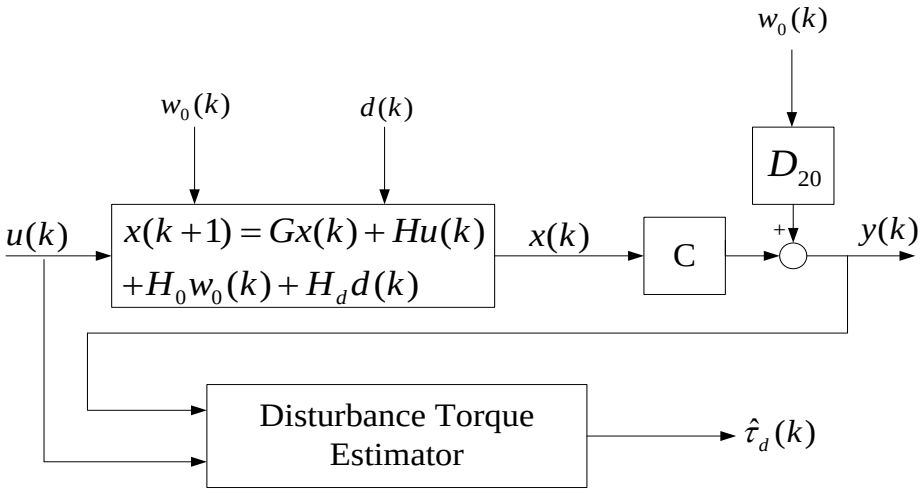

Figure 3- 3 System with Disturbance Torque Estimator using a Kalman Observer

Based on Equation 2-4 and Equation 3-20, the error dynamics of the estimator using a Kalman observer can be given as:

$$e(k+1) = x(k+1) - \hat{x}(k+1) \qquad (3\text{-}21)$$
$$= (G - LC)e(k) + (H_0 - LD_{20})w_0(k) + H_d\tau_d(k)$$

With the assumption that $H_0 w_0(k)$ and $D_{20} w_0(k)$ are zero-mean, uncorrelated white noises, the impact of those white noises are minimized by means of an observer gain L_{KD}. In other words, Equation 3-21 can be reduced to Equation 3-16 without loss of generality. Thus the estimator using a Kalman observer can estimate a constant or nearly constant disturbance torque under the condition that the system is subjected to white noises.

According to one of the assumptions of the Kalman observer, a prior knowledge of the covariance of the white noises is required. From this knowledge, H_0, and D_{20} can be obtained as $Q = H_0 H_0^T$ and $R = D_{20} D_{20}^T$, respectively. However, it is quite difficult to determine the covariances of these white noises. Hence, they are chosen by the designer as a design parameter in order to tune the estimation results.

3.3.3 H_∞ Observer

For a DC motor, model uncertainty is a common factor which affects the robustness of the system. In order to implement the H_∞ observer into the disturbance torque estimator, the system model of a DC motor should incorporate both model uncertainties and the disturbance torque. Figure 3-4 shows a system with disturbance torque estimator using an H_∞ observer.

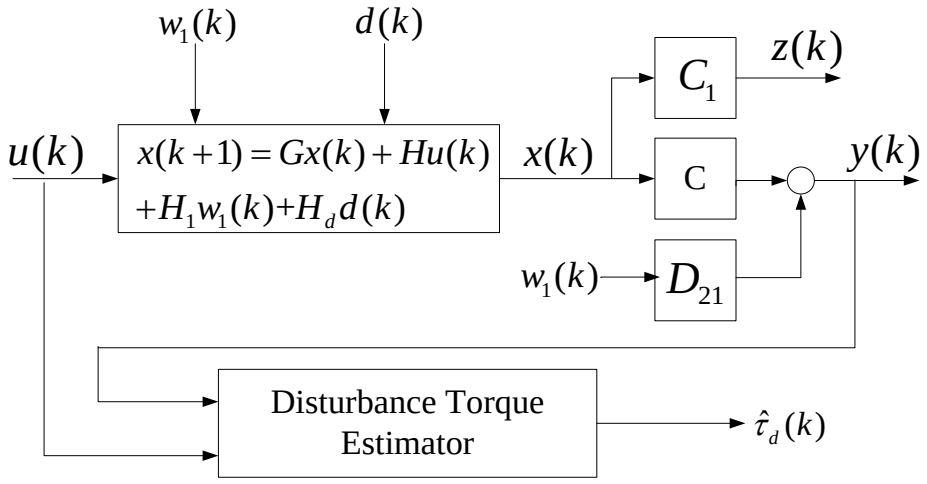

Figure 3-4 System with Disturbance Torque Estimator using an H_∞ Observer

For an H_∞ observer, the state space model of the DC motor is written as:

$$x(k+1) = Gx(k) + Hu(k) + H_1 w_1(k) + H_d d(k) \quad (3\text{-}22)$$

$$y(k) = Cx(k) + D_{21} w_1(k)$$

$$z(k) = C_1 x(k)$$

where $H_d = \begin{bmatrix} 0 \\ -\frac{T}{J_m} \end{bmatrix}$, $d(k) = \tau_d(k)$

and $w_1(k)$ is an uncertainty vector and H_1, D_{21} are weighting matrices describing the uncertainties and their significance. Depending on the types of uncertainties considered, $w_1(k), H_1,$ and D_{21} will be defined differently. It is noted that variations in model parameters and variations in measurement are treated as the model uncertainties for a DC motor drive system. The details of this will be discussed in Chapter 5

The error dynamics of the estimator using an H_∞ observer can be written as:

$$e(k+1) = x(k+1) - \hat{x}(k+1) \qquad (3\text{-}23)$$
$$= (G - LC)e(k) + (H_1 - LD_{21})w_1(k) + H_d\tau_d(k)$$

Since the objective of an H_∞ observer is to constrain the H_∞ norm of the transfer function from the estimation error to the uncertainty, Equation 3-23 can be reduced to Equation 3-16 without loss of generality. Thus, the estimator can achieve the robustness to model uncertainties by means of a steady-state observer gain L_{HID} while also being able to estimate both constant and low-frequency disturbance torques.

3.3.4 Mixed H_2/H_∞ Observer

In the case of the mixed H_2/H_∞ observer, both white noise and model uncertainty should be taken into account along with the disturbance torque in the DC motor model. A system with disturbance torque estimator using a mixed H_2/H_∞ observer is shown in Figure 3-5.

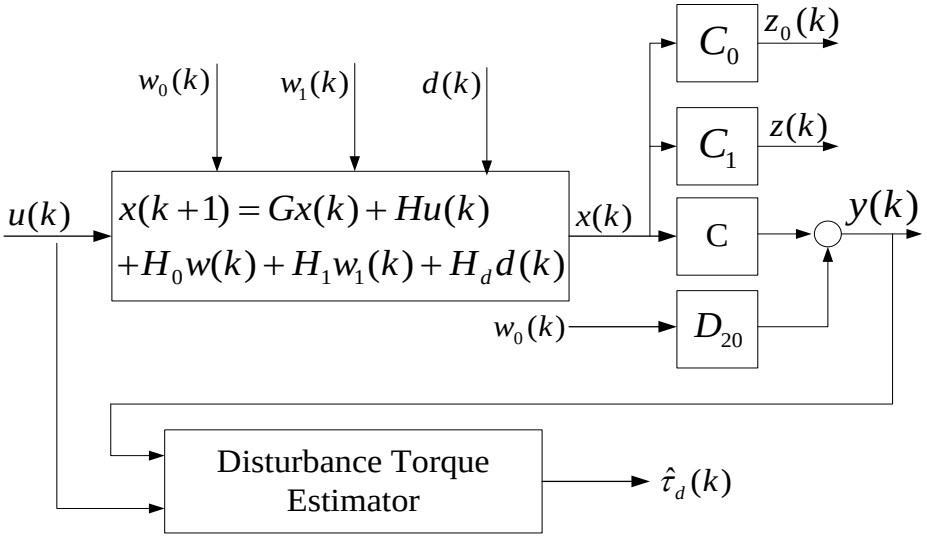

Figure 3-5 System with Disturbance Torque Estimator using a Mixed H_2/H_∞ Observer

For a mixed H_2/H_∞ observer, the state space model of the DC motor is formulated as:

$$x(k+1) = Gx(k) + Hu(k) + H_0 w_0(k) + H_1 w_1(k) + H_d d(k) \quad (3\text{-}24)$$

$$y(k) = Cx(k) + D_{20} w_0(k)$$

$$z(k) = C_1 x(k)$$

$$z_0(k) = C_0 x(k)$$

It can be seen in the above model that the measurement equation includes the noise vector $w_0(k)$ instead of the uncertainty vector $w_1(k)$. The reason for this incorporation is that the effect of the noise is more significant in the measurement branch. In addition, the matrix D_{11} is considered to be zero for the same reason as in the H_∞ Observer.

For a mixed H_2/H_∞ observer used in the disturbance torque estimator, the error dynamics can be given as

$$e(k+1) = x(k+1) - \hat{x}(k+1) \quad (3\text{-}25)$$

$$= (G - LC)e(k) + (H_0 - LD_{20})w_0(k) + H_1 w_1(k) + H_d \tau_d(k)$$

With the use a steady-state observer gain L_{MD}, the transfer function from uncertainty to error is constrained while the effect of white noise is minimized simultaneously. Thus the error dynamic shown above can be reduced to Equation 3-16, which means that the estimator using a mixed H_2/H_∞ observer can estimate a constant or low-frequency disturbance toque under the circumstance that both white noise and model uncertainty have an impact on the system.

3.3.5 H_/H$_\infty$ Observer

Although the H_/H$_\infty$ observer theory is originally presented for fault detection, it also provides one way of achieving multi-objective estimation of the disturbance torque. It can be seen in Equation 2-19 that $d(k)$ and $f(k)$ can be defined as different signals depending on specific condition. Thus, the state space model of a DC motor can be redefined as

$$x(k+1) = Gx(k) + Hu(k) + H_1 w_1(k) + H_d d(k) \quad (3\text{-}26)$$
$$y(k) = Cx(k) + D_{21} w_1(k)$$

In order to apply the multi-objective criteria into the estimator design, the external disturbance $d(k)$ and the internal disturbance caused by the model uncertainty $w(k)$ are defined as the two signals affecting the system. The objective is to make the estimation most sensitive to the disturbance signal and least sensitive to the model uncertainty.

Using Equation 2-4 and Equation 3-26, the error dynamics of the estimator using a H_/H$_\infty$ observer can be written as

$$e(k+1) = x(k+1) - \hat{x}(k+1) \quad (3\text{-}27)$$
$$= (G - LC)e(k) + (H_1 - LD_{21})w(k) + H_d d(k)$$

It can be seen in Equation 3-27 that the error dynamics are affected by the disturbance $d(k)$ and the model uncertainty $w(k)$ as well. As a result, the desired multi-objective observer should be designed to make the estimation most sensitive to the disturbance and least sensitive to the model uncertainty. This can be done using the H_/H$_\infty$ observer structure with the observer gain L_0. Then it can be assumed without loss of generality that Equation 3-27 can be reduced to Equation 3-16.

As mentioned previously, the output signal of the H_/H$_\infty$ observer structure is a residual signal $r(k)$ utilized to detect the fault. According to the algorithm, this residual signal has the most sensitivity to the disturbance and constrained sensitivity to uncertainty. For the purpose of applying H_/H$_\infty$ observer theory into the disturbance torque estimator, it is necessary to find a relationship between the disturbance torque estimation and the residual signal.

Equation 2-30 shows that the residual signal $r(k)$ can be calculated from the difference between the measurement output $y(k)$ and its estimation $\hat{y}(k)$. According to the model of the DC motor drive system in this thesis, the measurement output $y(k)$ is the armature current $I_a(k)$. Thus, the residual signal $r(k)$ can be described in the following form

$$r(k) = \gamma {R_d}^{-\frac{1}{2}} \left(I_a(k) - \hat{I}_a(k) \right) = \gamma {R_d}^{-\frac{1}{2}} e_i(k) \qquad (3\text{-}28)$$

With the finding that both the residual signal $r(k)$ and the disturbance torque estimation $\hat{\tau}_d(k)$ are related to the error in armature current $e_i(k)$, the H_/H$_\infty$ observer design for fault detection can be incorporated into a multi-objective disturbance torque estimator design. By reorganizing Equation 3-28 and substituting into Equation 3-14 we get

$$\hat{\tau}_d(k) = \left(K_t - \frac{L_{02} J_m}{T} \right) e_i(k) = \left(K_t - \frac{L_{02} J_m}{T} \right) \gamma^{-1} {R_d}^{1/2} r(k) \qquad (3\text{-}29)$$

where L_{02} is the element in the second row of the observer gain matrix L_0, which can be calculated using Equation 2-25 and Equation 2-26.

The H_/H$_\infty$ observer theory is thus fully implemented in the design of a multi-objective disturbance torque estimator.

CHAPTER 4

EXPERIMENTAL SETUP

4.1 Overview of the Hardware-in-the-Loop Testbench

Due to the fact that a real physical system is not ideal, the software simulation alone of a control algorithm is not enough to ensure whether it can satisfy some performance or robustness requirements. As a result, a hardware-in-the-loop (HIL) testbench is established to perform a real-time simulation of a design.

By using Simulink, the control algorithms or models to be tested are developed and then downloaded to an Opal-RT real-time computer. Then the HIL testbench can be used to perform a real-time simulation of the control algorithms or models. During the process of the HIL simulation, a communication with the physical components of the testbench is available. In detail, the user is allowed to monitor some sensor signals and data from the physical components and send control outputs as well.

A general layout of the HIL testbench is shown in Figure 4-1. With the use of some other physical components, the HIL testbench is established to test the disturbance torque estimator for a DC motor drive system. In order to test the performance and robustness of the estimator designs, different load disturbance torque conditions are provided during the

process of the HIL simulation. The configurations of major physical components will be detailed in the next section.

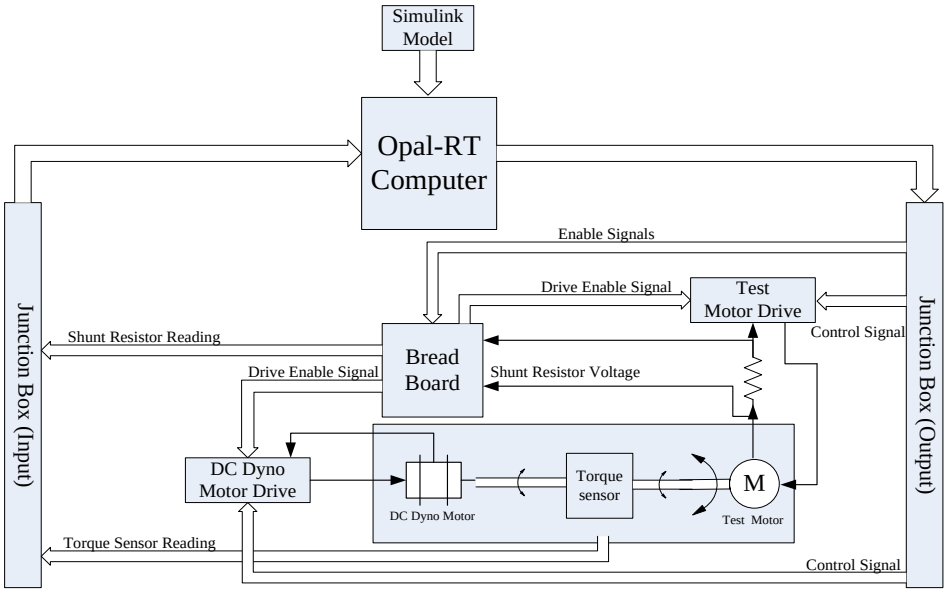

Figure 4-1 A general layout of the HIL testbench

4.2 Configurations of the Components

4.2.1 Motors

A Bosch GPA 12V 400W DC motor[22] is currently used to generate a low load torque, which can be treated as a load disturbance torque to the motor drive system. The Bosch motor used to provide disturbance torque to the test motor is shown in Figure 4-2.

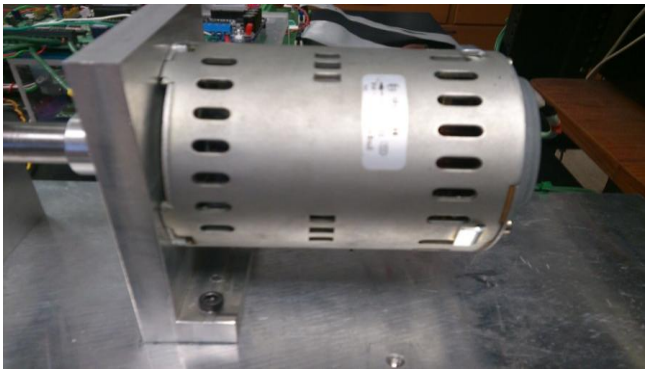

Figure 4-2 The Bosch Motor used to provide disturbance torque

A 24V Baldor DC motor[23] is currently used to test control algorithms and estimator designs. It can generate a full-load torque of 3 N-m. Originally, the Baldor motor was utilized to provide a load disturbance torque to the motor shaft. However, it is much more powerful than the Bosch motor, which makes it quite difficult to provide a relatively smaller load disturbance torque. As a result, the Baldor motor is used as the test motor in HIL testbench. Figure 4-3 shows the Baldor motor used to test the disturbance torque estimator.

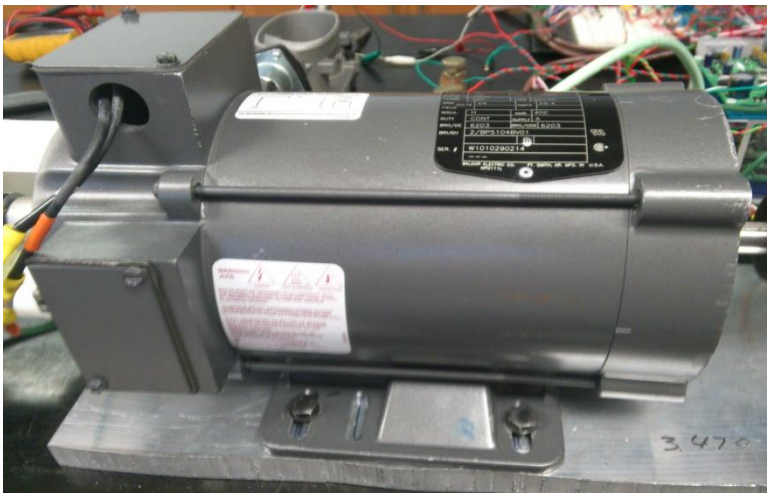

Figure 4-3 The Baldor Motor used to test the disturbance torque estimator

Since the Baldor motor is the test motor in the overall motor drive system, the knowledge of its parameters is essential due to the requirement of modeling. Based on the datasheet and experiment results, all of the necessary motor parameters are determined. The parameters will be detailed in the next chapter.

4.2.2 Motor Controllers Configurations

The Bosch motor is powered by a RoboteQ AX3500-BP motor drive[24]. It is a highly configurable, microcomputer-based, dual-channel digital speed or position controller with

built-in high power drivers. Figure 4-4 shows the wiring diagram for the Bosch motor controller.

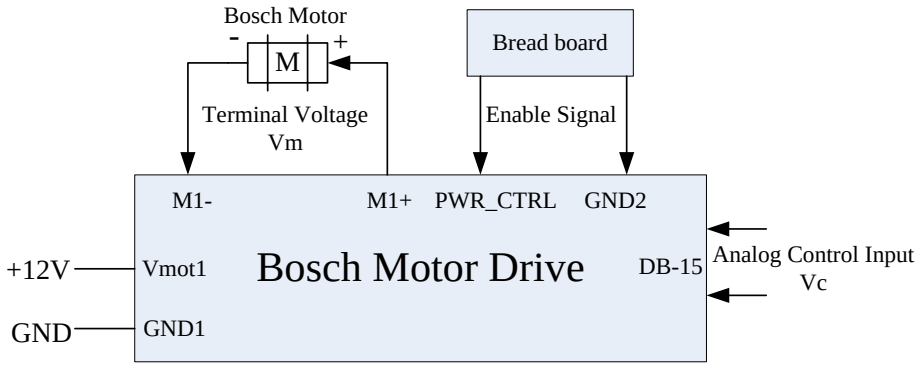

Figure 4-4 Wiring Diagram for the Bosch Motor Controller

It can be seen in Figure 4-4 that the Bosch motor controller is powered by a +12 VDC from a power supply. The Bosch motor is connected to the drive via an M+ and M- tabs pair. The PWR_CTRL tab with the GND2 tab are used to turn the controller on and off by means of an enable signal from the breadboard. The controller's I/O is a standard 15-pin D-Sub connector located on the board.

In the HIL testbench, the controller works in an open-loop, separate speed control mode. It delivers a power to the connected motor, which is proportional to the analog input voltage. The analog input voltage V_c is sent by the RT computer via the DB-15 connector, the controller will then generate a terminal voltage across the Bosch motor according to the following formula

$$V_m = -4.8V_c + 12 \qquad (4\text{-}1)$$

The Baldor motor is powered by a RoboteQ AX1500-BP DC motor controller[25]. Figure 4-5 shows the wiring diagram for the Baldor motor controller.

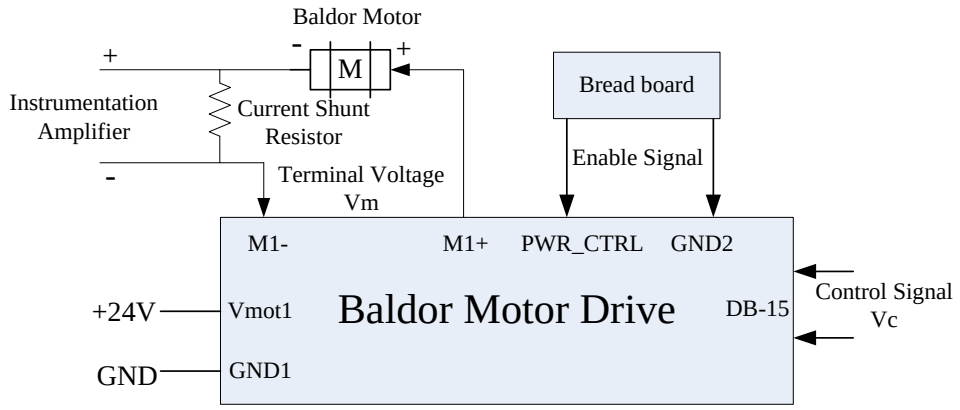

Figure 4-5 Wiring Diagram for the Baldor Motor Controller

Notice that most of the connections are the same as the Bosch motor drive with several exceptions. The controller is powered by a +24VDC from a power supply via the Vmot1 terminal and the GND1 terminal. In order to measure the armature current of the Baldor motor, a current shunt resistor is connected in series with the motor.

Similar to the Bosch motor controller, the Baldor motor controller also operates as an H-bridge that powers the motor in both directions. It converts the analog input voltage to a terminal voltage, which powers the connected motor. The relation between the analog input voltage and the terminal voltage is given as the following equation

$$V_m = -9.6V_c + 24 \qquad (4\text{-}2)$$

4.2.3 Current Shunt Resistor

In the HIL testbench, a current shunt resistor[26] is used as a sensor for armature current measurement. It has a nominal resistance of 0.25 mΩ, which is calculated from a 50mV rated voltage and a 200A rated current. As mentioned previously, the current shunt

resistor is connected in series with the Baldor motor such that all the armature current of the motor flows through the resistor. The voltage across the shunt resistor will be amplified by an instrumentation amplifier and then filtered by a low-pass RC filter.

In order to obtain the actual value of the armature current, some calculations are required. Since the signal read by the RT computer is an amplified, filtered voltage signal across the current shunt resistor, the actual value of the armature current can be given by diving the amplifier gain G_a and the nominal resistance of the shunt resistor using the follow formula:

$$I_a = \frac{V_o}{G_a R_{shunt}} = \frac{V_o}{122.12 * 0.0005} \quad (4\text{-}3)$$

where V_o is the signal read by the RT computer, G_a is the amplifier gain, R_{shunt} is the resistance of the current shunt resistance.

4.2.4 Torque Sensor

A torque sensor manufactured by Sensor Development is used in the HIL testbench for the purpose of validating the estimation results of the disturbance torque estimator. It is a standard strain gage sensor with an electronic circuit, which provides a DC excitation voltage[27]. The torque sensor is powered using a +12VDC and provides a mV/V output reflecting the torque applied to the shaft. Figure 4-6 shows the mounting of the torque sensor with the motors.

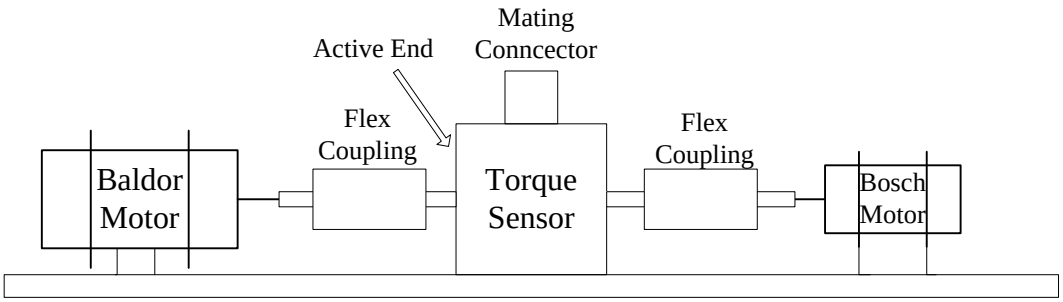

Figure 4-6 Mounting of the Torque Sensor with the Motors

It is noted that the torque sensor in the HIL testbench has a label "Active End" [28]on one side, which is a very important issue during the installation. According to the document of the manufacturer, the "Active End" should be facing the place where torque needs to be measured. Hence, to measure the disturbance torque provided by the Bosch motor, the torque sensor should be mounted as the way shown in Figure 4-6.

Due to the feature mentioned above, only the torque applied to the right of the torque sensor can be measured. A problem thus arises that the measurement of the torque sensor is not equal to the disturbance torque acting on the whole shaft. Based on the experiments, the flux couplings are proved to have an impact on the torque. However, the torque sensor takes the effect of the right coupling into account while ignores that of the left coupling. As a result, a compensation may be required to make the torque sensor reflect a more accurate measurement. Based on the datasheet of the torque sensor and results of experiments, the following formula is used to convert the output voltage of the sensor to a torque value.

$$T_{Load} = (0.7243 + 0.00007 * V_{out}) * V_{out} \quad (4\text{-}4)$$

4.2.5 Opal-RT Real-Time Computer

An RT computer is used as the target node during the process of the HIL simulation, which plays a role as a real-time processing and communication computer. In general, the RT computer performs real-time execution of the model's simulation, real-time communications with I/Os, acquisitions of the model's internal variables and external outputs through I/Os, and implementation of user's online parameters modification[29].

4.2.6 Command Station

A Dell PC workstation is used as a command station in the HIL testbench. By using the software Simulink, the model for simulation can be developed and edited on the command station. In addition, the user can compile the simulation model, download the model to the RT computer, and interact with the physical components during the real-time simulation.

4.3 RT-LAB

RT-Lab is a software package for engineer who use mathematical block diagrams for simulation, control, and related applications.[29] In the HIL testbench, a RT-Lab main control panel is installed on the command station, which allows the user to access easily the RT-Lab functions. Figure 4-7 shows the graphic user interface (GUI) of the RT-Lab main control panel.

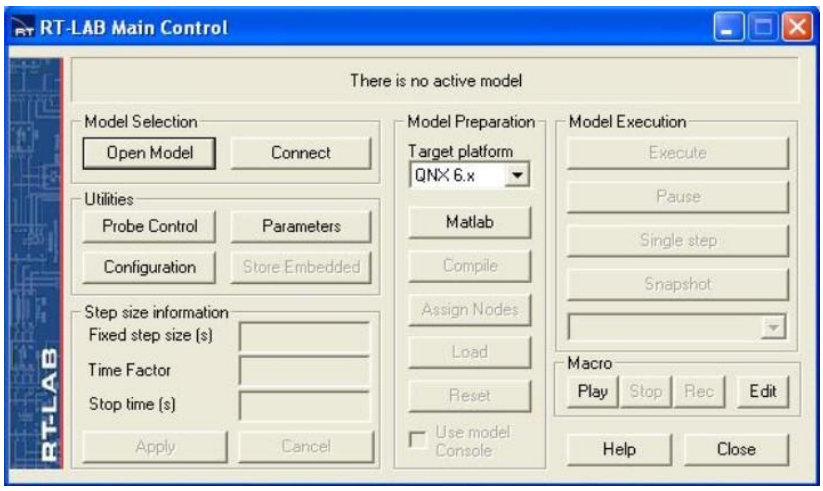

Figure 4-7 GUI of the RT-Lab Main Control Panel

According to the above GUI, the main functions the panel offers include opening the Simulink model, compiling the model and generating codes, loading the model to the RT computer, starting or pausing the model's simulation, and restarting the system.

The entire process of the HIL simulation using RT-Lab can be summarized as the following steps:

1. Turn on the RT computer and the command station and make sure that they are connected via a LAN cable.
2. Connect and turn on the physical components required for the HIL simulation.
3. Develop the Simulink model and group the model into two subsystems based on the requirements of RT-LAB.
4. Use the control panel to open the Simulink model, compile the model, and load to the RT computer.
5. Execute the simulation and interact with the physical components of the test bench.

CHAPTER 5

TEST RESULTS

In order to verify that the performance and robustness requirements are satisfied, all of the estimator designs are tested using a DC motor (Baldor motor) attached to a dyno moto r (Bosch motor) in the HIL testbench. The parameters of the DC motor are listed in Table 5-1. Since all the estimators are capable of estimating a constant or low-frequency torque, different load disturbance torques are provided by the dyno motor. An in-line torque sensor in the testbench provides an actual measurement of the disturbance torque, which is used to validate the estimation.

Rated Voltage	24 V
Rated Current	29.4 A
Rated Speed	1800 RPM
Rated Power	0.75 hp
Armature Resistance	0.0933 Ω
Armature Inductance	0.000749 H
Electrical Constant	0.11235 V/rad/s
Mechanical Constant	0.11235 N-m/A
Inertial Coefficient	1.8078×10^{-4} kg/m^2
Viscous Friction Coefficient	1.2404×10^{-3} N-m/rad/s

Table 5-1 Parameters of the Test Motor

5.1 Disturbance Torque Estimation using Kalman Observer

For the disturbance torque estimator using a Kalman observer, the noise vector and covariance matrices are defined as

$$w_0 = \begin{bmatrix} V_{brush} \\ \Delta I_a \end{bmatrix}, \qquad H_0 = \begin{bmatrix} \frac{w_{01}}{L_a} & 0 \\ 0 & 0 \end{bmatrix} T, \qquad D_{20} = [0 \quad w_{02}]$$

where w_{01}, w_{02} are positive constants that represent noise covariances and can be used to determine the observer gain. The parameters and the resulting observer gain are listed in Table 5-2.

w_{01}	1
w_{02}	1
L_{KD}	$\begin{bmatrix} -8.4299 \times 10^{-2} \\ 1.4562 \times 10^{0} \end{bmatrix}$

Table 5-2 Parameters for Kalman Observer Gain Calculation and the Resulting Gain

A disturbance torque signal consisting of step signals, sawtooth wave signals and sinewave signals is used to test the estimator design incorporating the Kalman observer. Figure 5-1 shows the overall test results of the Kalman disturbance torque estimation.

Since the Kalman observer is designed to reject white noise, some results should also be acquired to verify if this requirement is satisfied. These results for the Kalman disturbance torque estimation are shown in Figure 5-2.

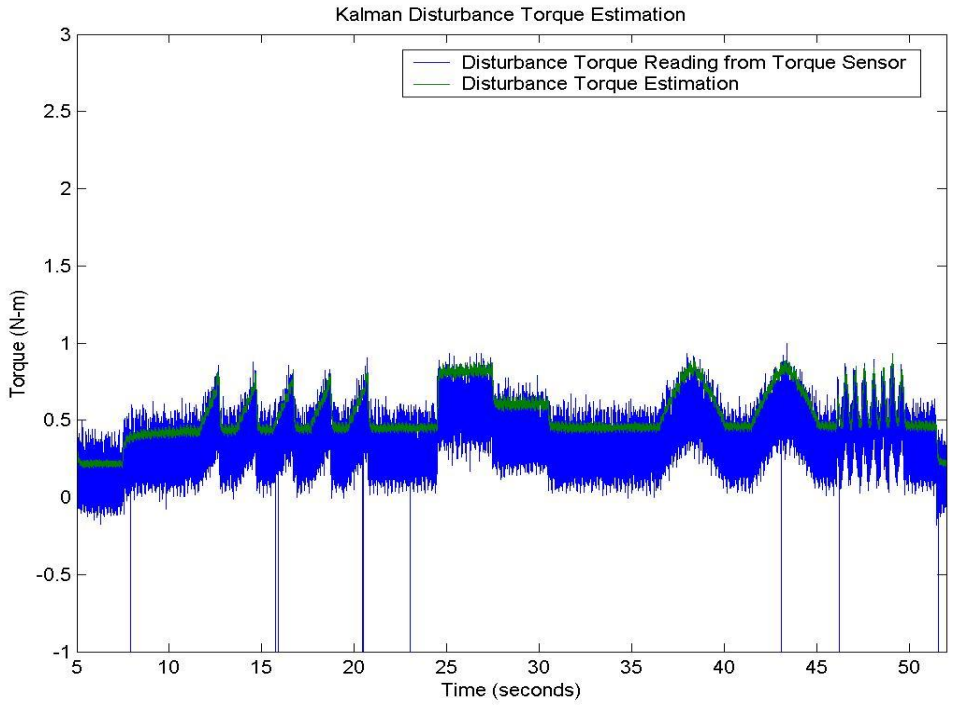

Figure 5-1 Overall Test Results of Kalman Disturbance Torque Estimation

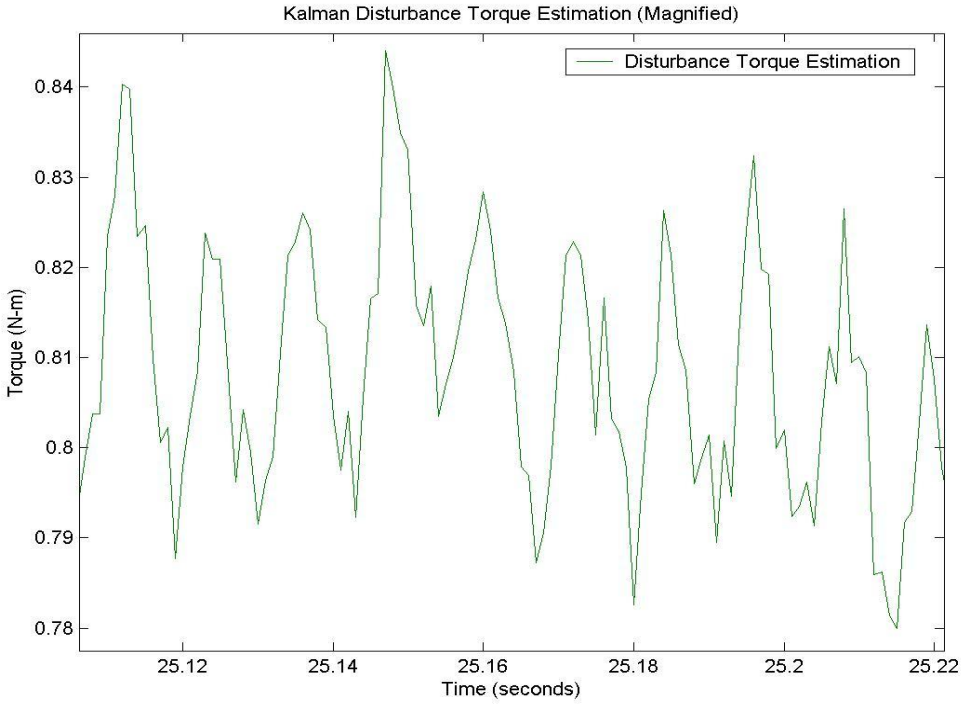

Figure 5-2 Noise Test Results of Kalman Disturbance Torque Estimation

According to Figure 5-1, it can be seen that the estimator using the Kalman observer is capable of delivering an estimation for both constant and low-frequency disturbance torques. It can also be seen in Figure 5-2 that the estimation contains little noise since it has minimal high-frequency components and a small amount of variations. Thus, the estimator using the Kalman observer is verified to achieve an appropriate estimation and noise rejection. The estimation results may be improved by tuning the parameters listed in Table 5-1.

5.2 Disturbance Torque Estimation using H_∞ Observer

Since an H_∞ observer is designed to be robust to model uncertainties, there is a need to test the estimator design with respect to various combinations of model uncertainties. For a DC motor, model uncertainties are mostly resulted from the variations in the electrical parameters such as R_a, K_v, and L_a. Due to the assumption that the disturbance torque is a constant or low-frequency signal, the effect of ΔL_a can be ignored. Thus ΔR_a, ΔK_v are the only two parameters of interest.

Apart from the two electrical parameters, ΔI_a is considered to be measurement uncertainty. The primary reason for this is to ensure that the DARE used for the observer gain calculation has a solution.

In addition, ΔI_a is used to reflect the measurement uncertainty since the accuracy of the

armature current measurement cannot be guaranteed in a real physical system. As mentioned previously, the armature current is obtained by using a current shunt resistor which is connected in series with the test motor. Thus, the shunt resistance and its variation will have an impact on the value of armature current measurement. As a result, it is necessary to consider the variation in the armature current as a model uncertainty.

Using ΔR_a, ΔK_v and ΔI_a, three cases can be defined. The vector w_1 is used to represent the model uncertainties and H_1, D_{21} are two weighting matrices that describe how significantly the model uncertainties affect the system.

Case 1 $$w_1 = \begin{bmatrix} \Delta R_a I_a \\ \Delta I_a \end{bmatrix},\ H_1 = \begin{bmatrix} -\frac{w_{11}}{L_a} & 0 \\ 0 & 0 \end{bmatrix} T,\ D_{21} = [0 \quad w_{13}]$$

Case 2 $$w_1 = \begin{bmatrix} \Delta K_v \omega_m \\ \Delta I_a \end{bmatrix},\ H_1 = \begin{bmatrix} -\frac{w_{12}}{L_a} & 0 \\ 0 & 0 \end{bmatrix} T,\ D_{21} = [0 \quad w_{13}]$$

Case 3 $$w_1 = \begin{bmatrix} \Delta R_a I_a \\ \Delta K_v \omega_m \\ \Delta I_a \end{bmatrix},\ H_1 = \begin{bmatrix} -\frac{w_{11}}{L_a} & -\frac{w_{12}}{L_a} & 0 \\ 0 & 0 & 0 \end{bmatrix} T,\ D_{21} = [0 \quad 0 \quad w_{13}]$$

In all cases, w_{11}, w_{12}, and w_{13} are some positive weight parameters that describe the significance of the particular uncertainty. The weight parameters for all three cases and the resulting observer gains are listed in Table 5-3

	w_{11}	w_{12}	w_{13}	γ	L_{HID}
Case1	1	N/A	1	5	$\begin{bmatrix} 1.0613 \times 10^{0} \\ -1.0225 \times 10^{-2} \end{bmatrix}$
Case2	N/A	0.7	1	3	$\begin{bmatrix} 1.1104 \times 10^{0} \\ 4.1296 \times 10^{-1} \end{bmatrix}$
Case3	0.5	0.5	1	5	$\begin{bmatrix} 1.1143 \times 10^{0} \\ 4.0617 \times 10^{-1} \end{bmatrix}$

Table 5-3 Parameters for H_∞ Observer Gain Calculation and the Resulting Gains

Each case is tested using a nominal plant model, a -10% variation of the particular parameter, and a +10% variation of the particular parameter.

The overall test results of the H_∞ disturbance torque estimation case 1 is shown in Figure 5-3. A disturbance torque signal consisting of step signals, sawtooth signals, and sinewave signals is used to verify if the estimator is capable of delivering an estimation of both constant and low-frequency disturbance torques. The results of the estimations are validated with an in-line torque sensor.

For the purpose of showing robustness, the estimations using nominal armature resistance and ±10% variation of the armature resistance are magnified. These results are shown in Figure 5-4. In addition, the estimation using nominal parameters is also magnified in Figure 5-5 to show the performance of this observer towards noise rejection.

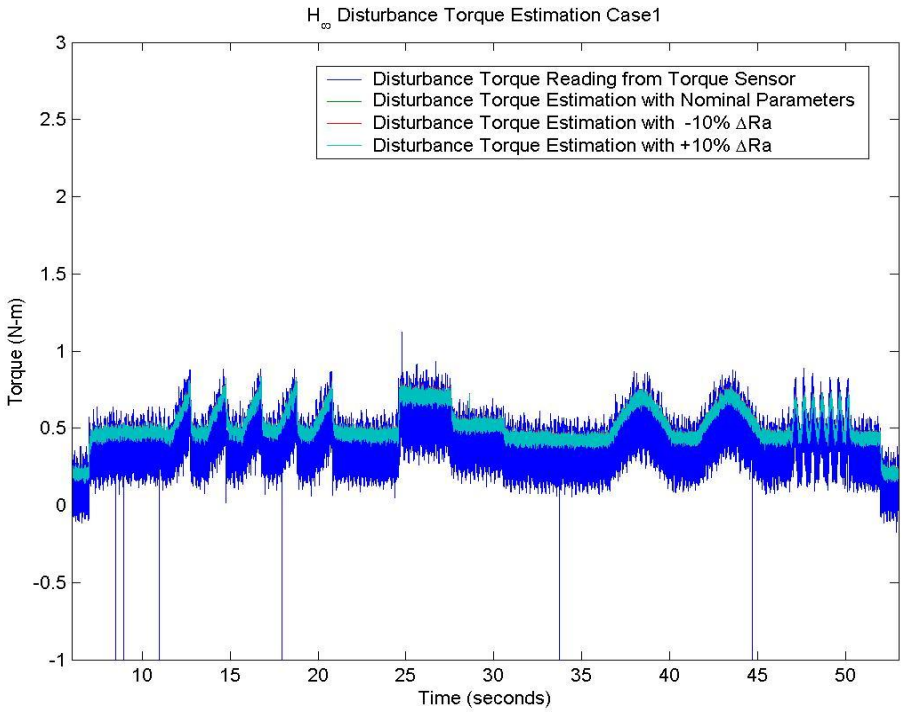

Figure 5-3 Overall Test Results of H_∞ Disturbance Torque Estimation Case 1

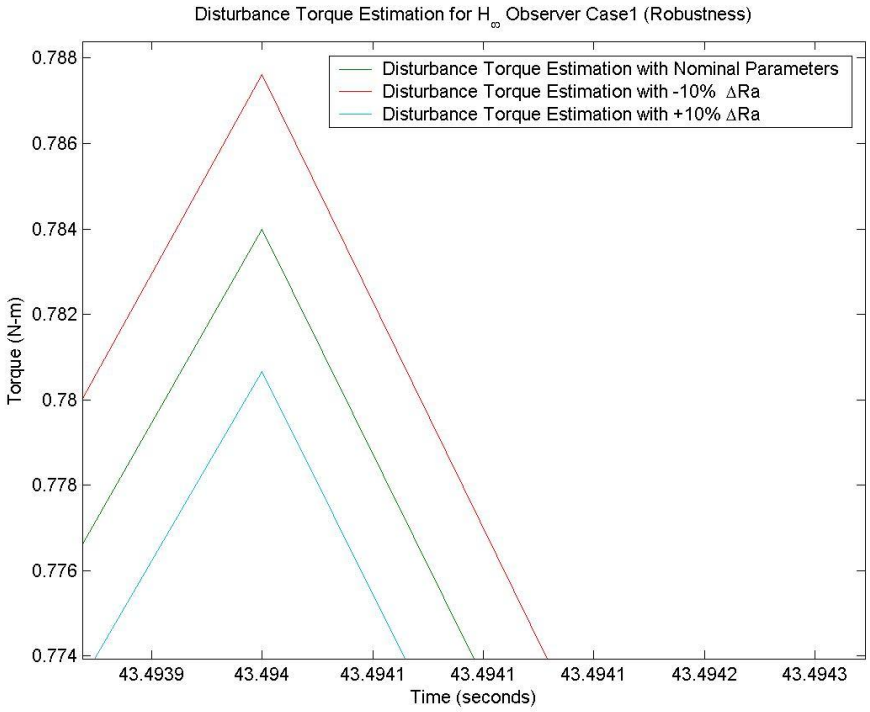

Figure 5-4 Robustness Test Results of H_∞ Disturbance Torque Estimation Case 1

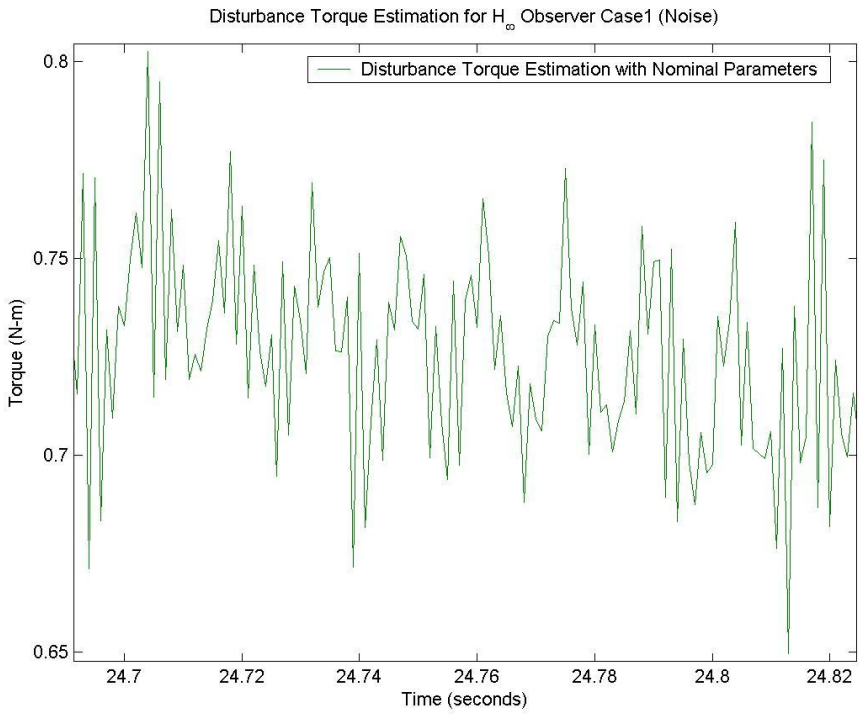

Figure 5-5 Noise Test Results of H_∞ Disturbance Torque Estimation Case 1

According to the results shown in Figure 5-3, the estimator using the H_∞ observer can generate an estimation for both constant and low-frequency disturbance torques when the system is subjected to variations in armature resistance. It can also be seen in Figure 5-4 that the variation between the estimation using nominal armature resistance and ±10% variation of the armature resistance is negligibly small. Hence, it is verified that the H_∞ disturbance estimation is robust to the variations in the armature resistance. Figure 5-5 shows that the estimation has more high-frequency components and larger magnitude of variations making it noisy. This is expected since the H_∞ observer does not consider the effect of white noise in its observer algorithm. Similar results for case 2 and case 3 are shown in Figure 5-6, 5-7, 5-8 and Figure 5-9, 5-10, 5-11, respectively.

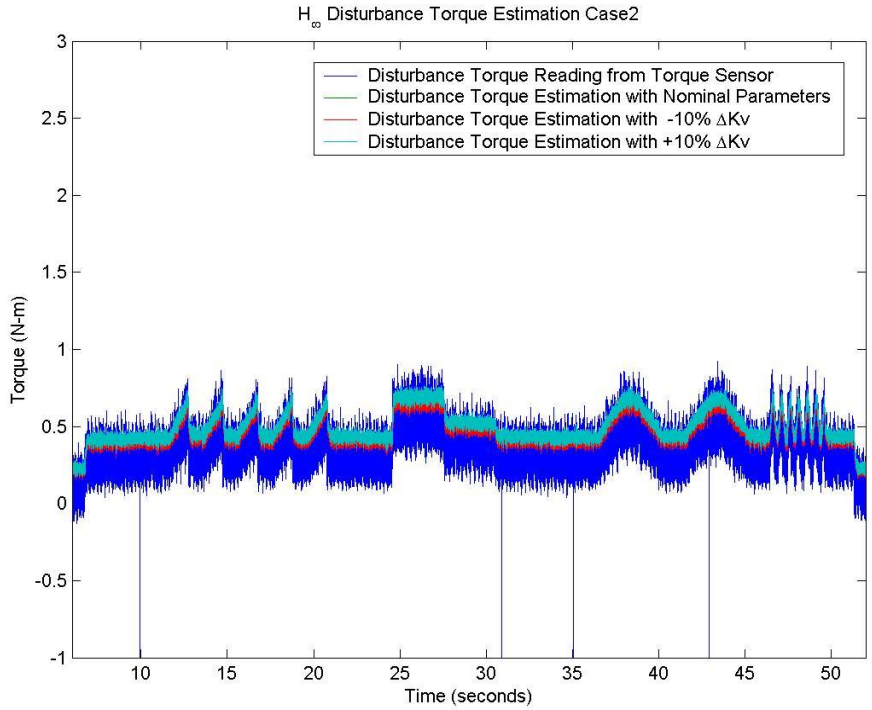

Figure 5-6 Overall Test Results of H_∞ Disturbance Torque Estimation Case 2

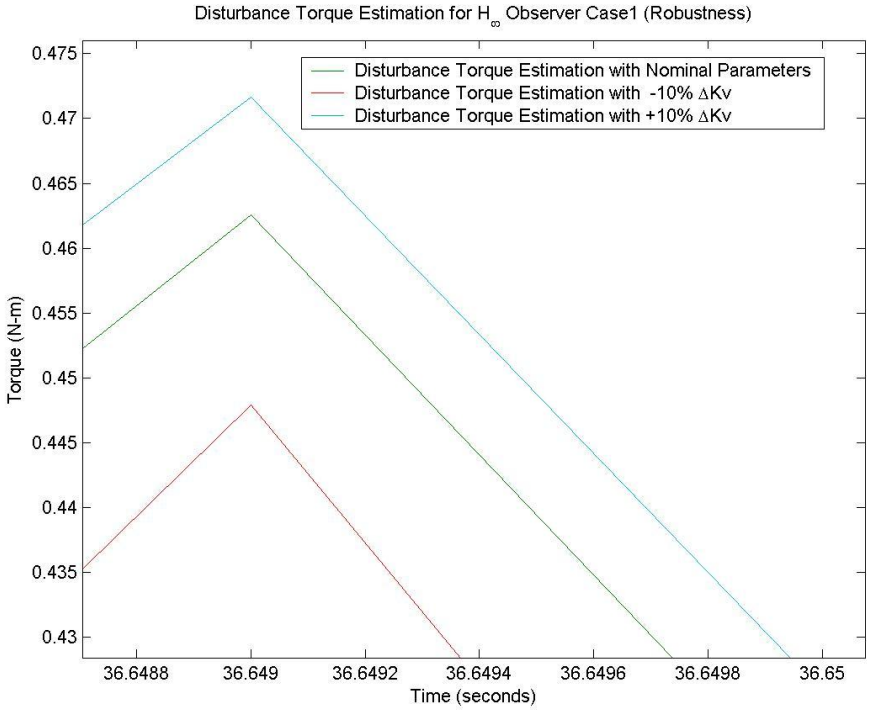

Figure 5-7 Robustness Test Results of H_∞ Disturbance Torque Estimation Case 2

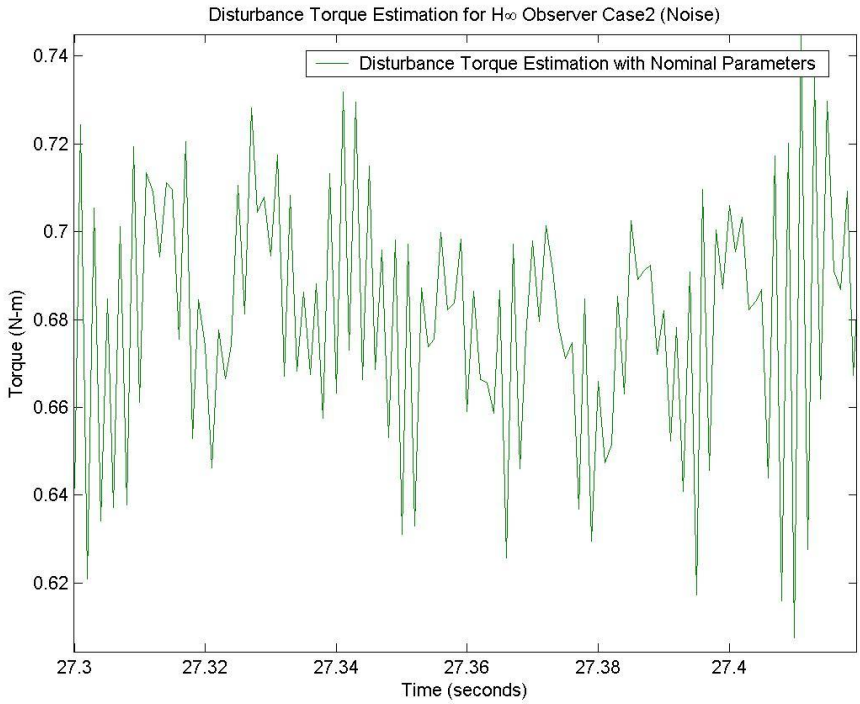

Figure 5-8 Noise Test Results of H_∞ Disturbance Torque Estimation Case 2

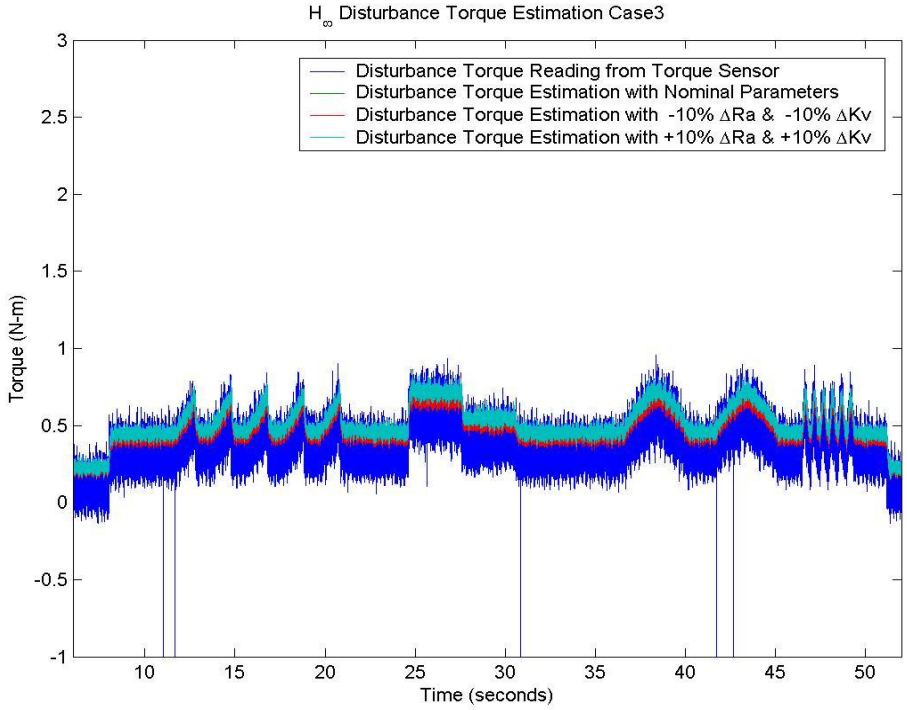

Figure 5-9 Overall Test Results of H_∞ Disturbance Torque Estimation Case 3

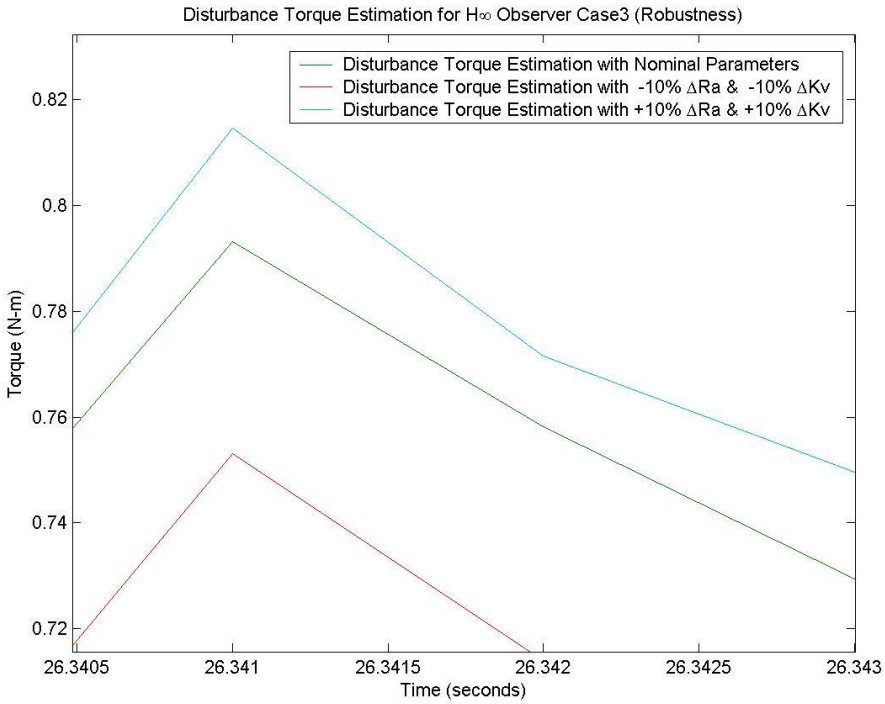

Figure 5-10 Robustness Test Results of H_∞ Disturbance Torque Estimation Case 3

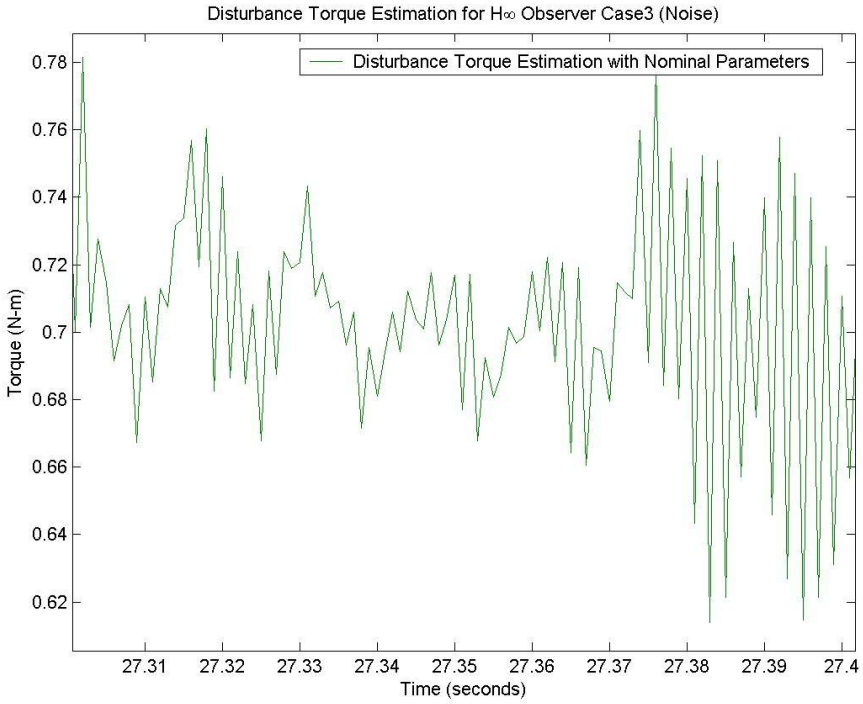

Figure 5-11 Noise Test Results of H_∞ Disturbance Torque Estimation Case 3

Based on the results shown previously, the estimator using the H_∞ observer is capable of estimating both constant and low-frequency disturbance torques while achieving robustness to all the three cases of model uncertainties. Further improvement of the estimation may be done by tuning the parameters listed in Table 5-3 and the matrix S in (2-11) and (2-12).

5.3 Disturbance Torque Estimation using Mixed H_2/H_∞ Observer

Similar to the H_∞ observer, three separate cases are also defined to represent various combinations of model uncertainties and white noises.

Case 1

$$w_0 = \begin{bmatrix} V_{brush} \\ \Delta I_a \end{bmatrix}, H_0 = \begin{bmatrix} \frac{w_{01}}{L_a} & 0 \\ 0 & 0 \end{bmatrix} T, D_{20} = [0 \quad w_{02}], w_1 = [\Delta R_a I_a],\ H_1 = \begin{bmatrix} -\frac{w_{11}}{L_a} \\ 0 \end{bmatrix} T$$

Case2

$$w_0 = \begin{bmatrix} V_{brush} \\ \Delta I_a \end{bmatrix}, H_0 = \begin{bmatrix} \frac{w_{01}}{L_a} & 0 \\ 0 & 0 \end{bmatrix} T, D_{20} = [0 \quad w_{02}], w_1 = [\Delta K_v \omega_m],\ H_1 = \begin{bmatrix} -\frac{w_{12}}{L_a} \\ 0 \end{bmatrix} T$$

Case 3

$$w_0 = \begin{bmatrix} V_{brush} \\ \Delta I_a \end{bmatrix}, H_0 = \begin{bmatrix} \frac{w_{01}}{L_a} & 0 \\ 0 & 0 \end{bmatrix} T, D_{20} = [0 \quad w_{02}] w_1 = \begin{bmatrix} \Delta R_a I_a \\ \Delta K_v \omega_m \end{bmatrix},\ H_1 = \begin{bmatrix} -\frac{w_{11}}{L_a} & -\frac{w_{12}}{L_a} \\ 0 & 0 \end{bmatrix} T$$

In all cases, w_{11}, w_{12} are weight parameters representing the significance of the model uncertainties and w_{01}, w_{02} are some positive constants that represent covariances of white noises. The parameters for all cases and the corresponding observer gains are listed in Table 5-4.

	w_{01}	w_{02}	w_{11}	w_{12}	γ	L_{MD}
Case1	0.5	1	0.2	N/A	10	$\begin{bmatrix} -6.9828 \times 10^{-2} \\ 1.3662 \times 10^{0} \end{bmatrix}$
Case2	0.2	1	N/A	0.1	20	$\begin{bmatrix} -3.9019 \times 10^{-2} \\ 9.7899 \times 10^{-1} \end{bmatrix}$
Case3	0.1	1	0.1	0.1	20	$\begin{bmatrix} -1.3675 \times 10^{-2} \\ 5.1823 \times 10^{-1} \end{bmatrix}$

Table 5-4 Parameters for Mixed H_2/H_∞ Observer Gain Calculation and the Resulting Gains

Each case is tested using a nominal plant model, a -10% variation of the particular parameter, and a +10% variation of the particular parameter.

Similar to the H_∞ disturbance torque estimation, the estimator design using the mixed H_2/H_∞ observer is also tested to verify if an appropriate estimation, robustness to model uncertainty, and noise rejection can be achieved.

Figure 5-12 shows the overall test results of the estimator using the mixed H_2/H_∞ observer. Test results of the estimation using the nominal armature resistance and ±10% variation of the armature resistance are shown in Figure 5-13. These estimation results are magnified in order to verify the robustness of the estimation to the model uncertainty (case 1). In Figure 5-14, the magnified results of the estimation using the nominal parameter show the level of noise in the estimation.

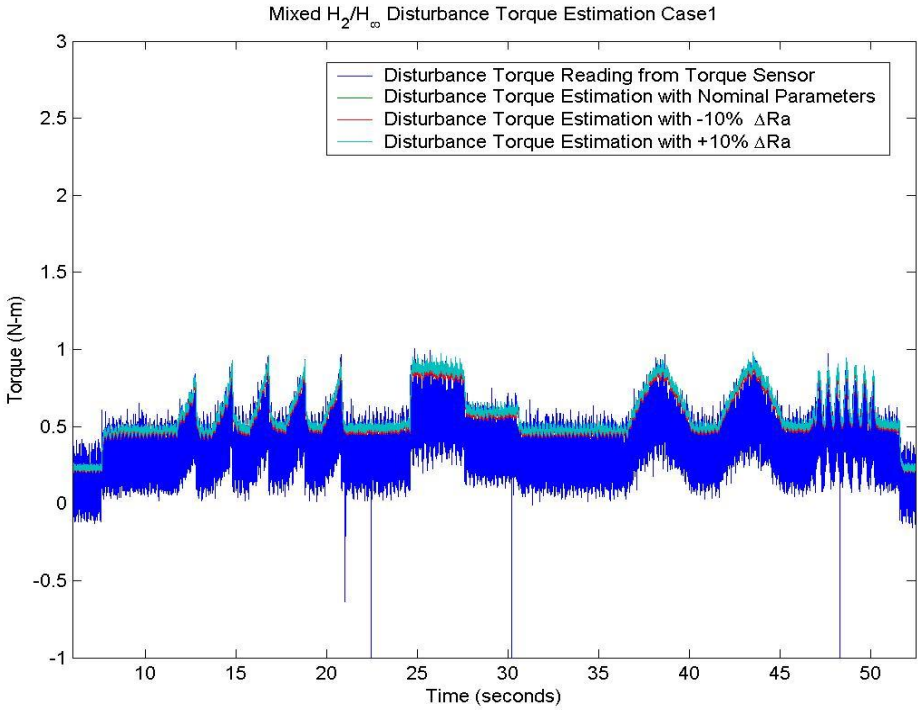

Figure 5-12 Overall Test Results of Mixed H_2/H_∞ Disturbance Torque Estimation Case 1

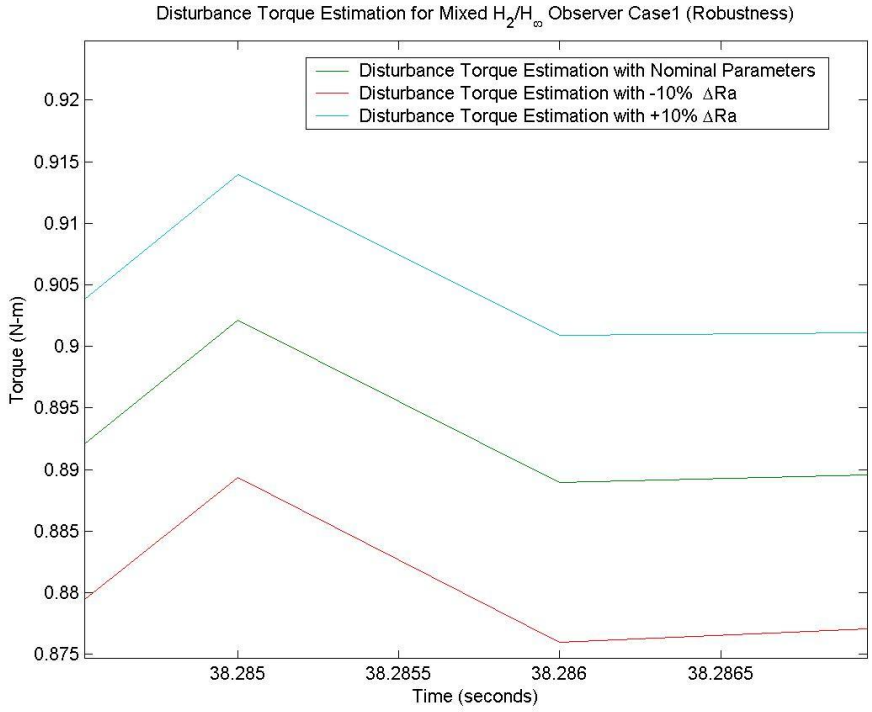

Figure 5-13 Robustness Test Results of Mixed H_2/H_∞ Disturbance Torque Estimation Case 1

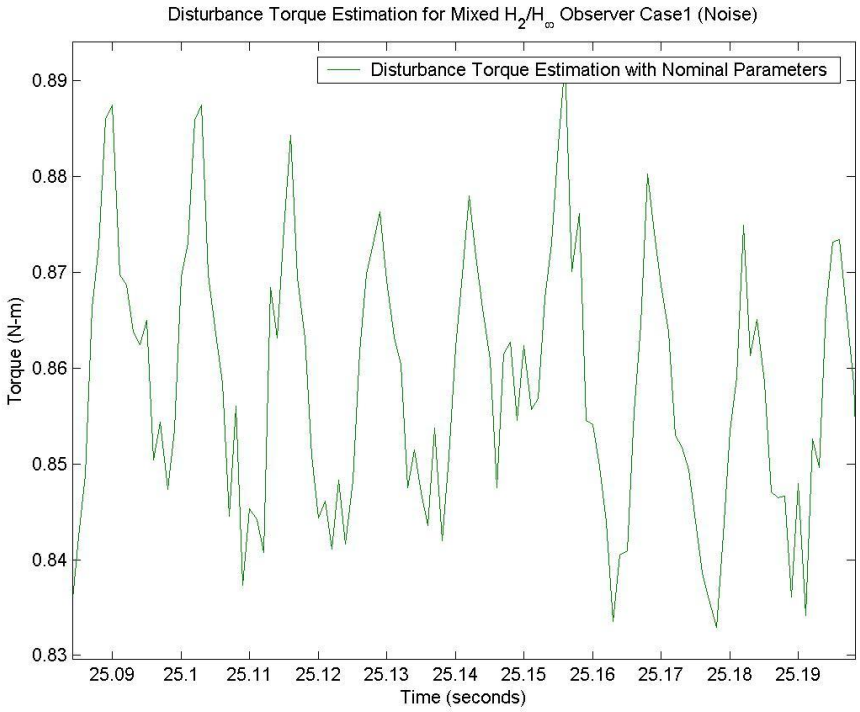

Figure 5-14 Noise Test Results of Mixed H_2/H_∞ Disturbance Torque Estimation Case 1

It can be seen in Figure 5-12 that the estimator using the mixed H_2/H_∞ observer can achieve appropriate estimations for both constant and low-frequency disturbance torques. Based on the test results shown in Figure 5-13, it can also be seen that the variations between the estimations are small and negligible and thus verify the robustness of the estimation to the variations in armature resistance. In comparison to Figure 5-5, it can be seen clearly that the test results shown in Figure 5-14 have fewer high-frequency components and less variations. This is expected since the mixed H_2/H_∞ observer is designed to achieve both white noise rejection and model uncertainty attenuation.

Similar results for case 2 and case 3 are shown in Figure 5-15, 5-16, 5-17 and Figure 5-18, 5-19,5-20, respectively.

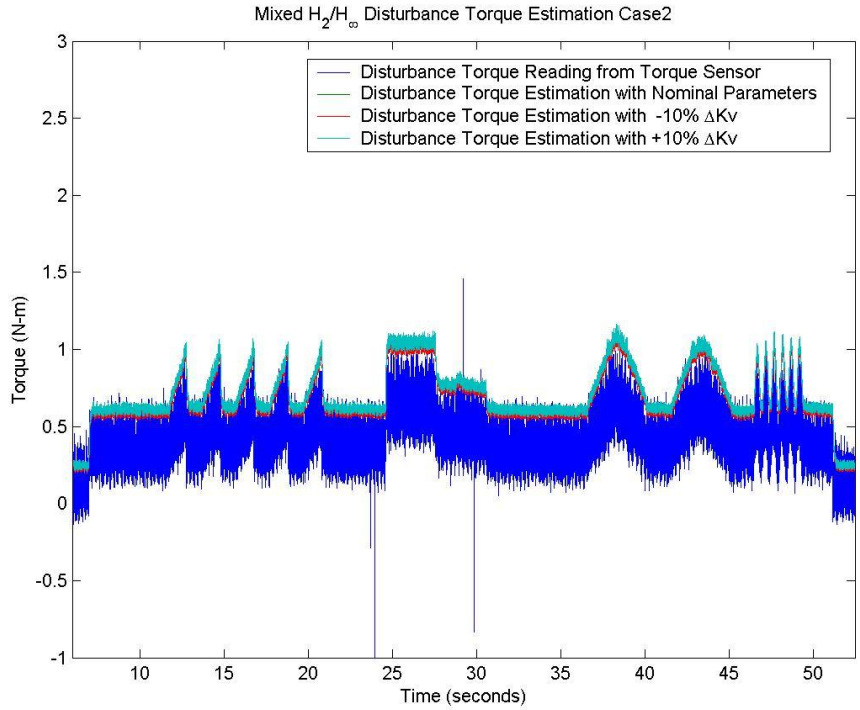

Figure 5-15 Overall Test Results of Mixed H_2/H_∞ Disturbance Torque Estimation Case 2

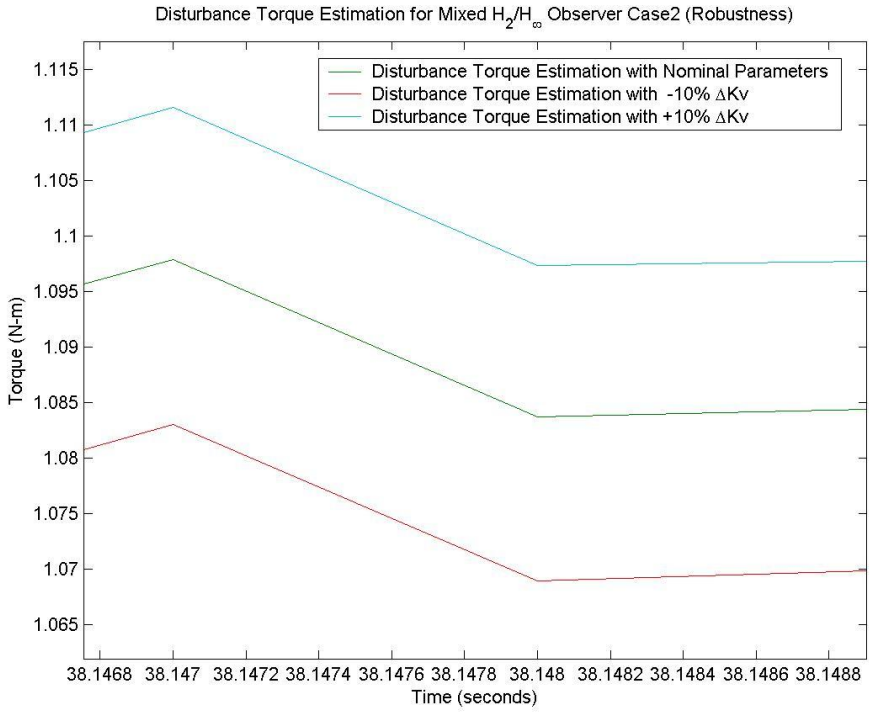

Figure 5-16 Robustness Test Results of Mixed H_2/H_∞ Disturbance Torque Estimation Case 2

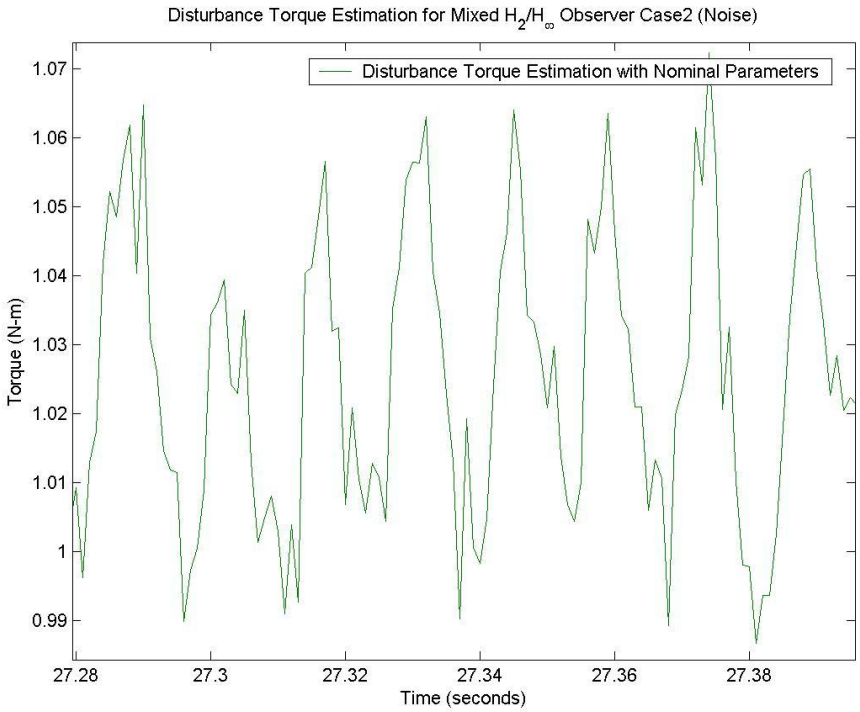

Figure 5-17 Noise Test Results of Mixed H_2/H_∞ Disturbance Torque Estimation Case 2

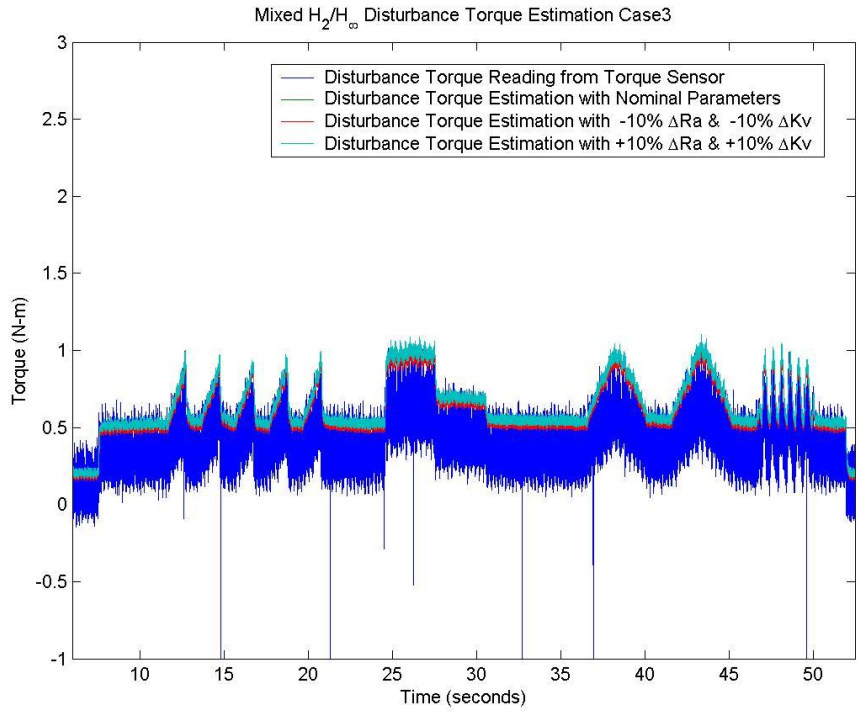

Figure 5-18 Overall Test Results of Mixed H_2/H_∞ Disturbance Torque Estimation Case 3

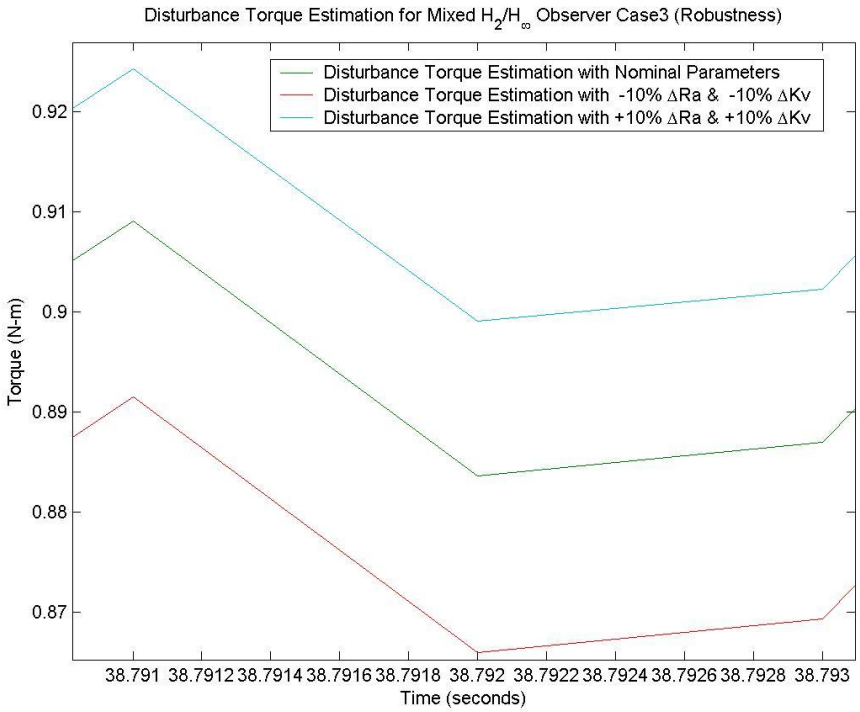

Figure 5-19 Robustness Test Results of Mixed H_2/H_∞ Disturbance Torque Estimation Case 3

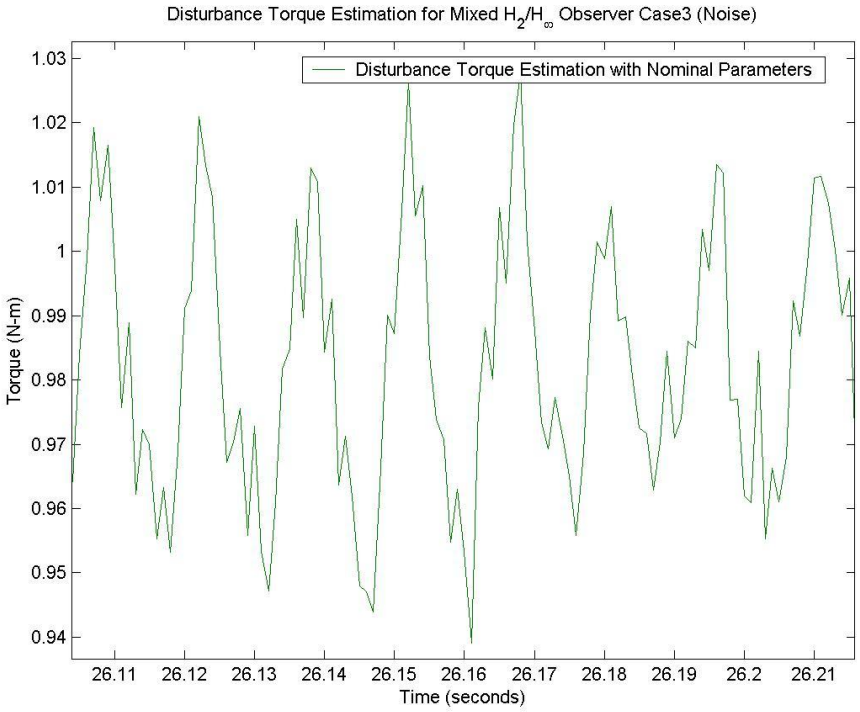

Figure 5-20 Noise Test Results of Mixed H_2/H_∞ Disturbance Torque Estimation Case 3

In comparison to the estimation results of the H_∞ observer, it can be seen clearly that the estimator using a mixed H_2/H_∞ observer can achieve robust estimation with little noise. By tuning the parameters listed in Table 5-4, a better trade-off between noise rejection and uncertainty attenuation may be found.

5.4 Disturbance Torque Estimation using H_-/H_∞ Observer

In the case of the H_-/H_∞ observer, the estimator is designed to be most sensitive to the disturbance torque and least sensitive to the model uncertainty. As a result of the multi-objective criteria, three cases of uncertainties are defined exactly the same as the H_∞ observer. The parameters for all three cases and observer gains are listed in Table 5-5.

	w_{11}	w_{12}	w_{13}	γ	L_{HID}
Case1	1	N/A	0.01	10	$\begin{bmatrix} -8.8441 \times 10^{-2} \\ 1.4899 \times 10^{0} \end{bmatrix}$
Case2	N/A	0.1	1	10	$\begin{bmatrix} -1.3942 \times 10^{-2} \\ 5.1690 \times 10^{-1} \end{bmatrix}$
Case3	0.1	0.1	1.5	10	$\begin{bmatrix} -1.2531 \times 10^{-2} \\ 4.8067 \times 10^{-1} \end{bmatrix}$

Table 5-5 Parameters for H_-/H_∞ Observer Gain Calculation and the Resulting Gains

Each case is tested using a nominal plant model, a -10% variation of the particular parameter, and a +10% variation of the particular parameter.

For case 1, the overall test results of the estimator design using the H_-/H_∞ observer are shown in Figure 5-21. The estimation using the nominal armature resistance and ±10% variation of the armature resistance are shown in Figure 5-22.

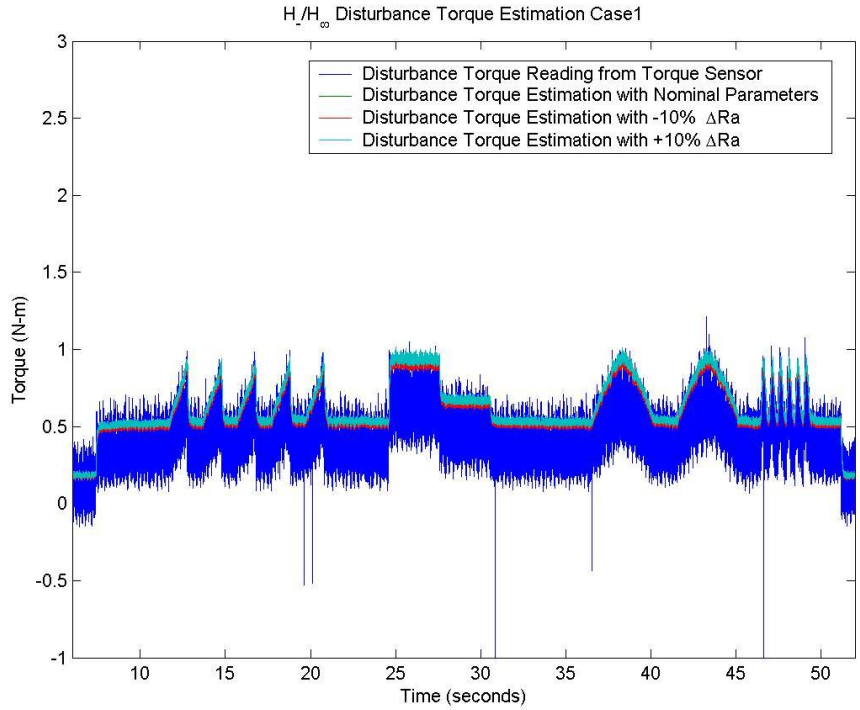

Figure 5-21 Overall Test Results of H_/H∞ Disturbance Torque Estimation Case 1

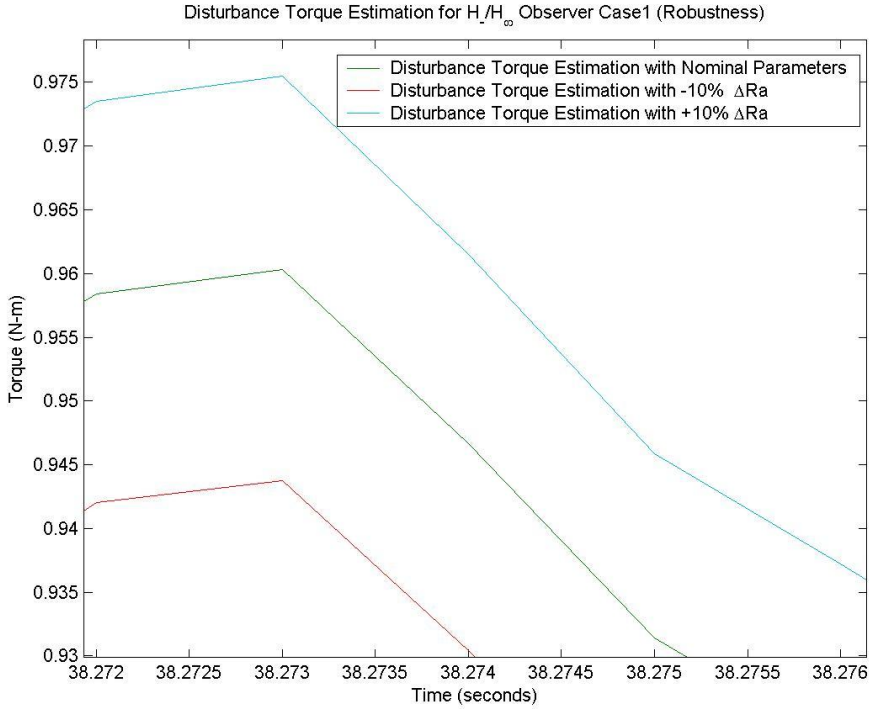

Figure 5-22 Robustness Test Results of H_/H∞ Disturbance Torque Estimation Case 1

Apart from verifying appropriate estimation results and robustness, the sensitivity of the estimation to the disturbance torque should also be verified. For this purpose, a staircase signal increasing in small increments is used as the disturbance torque and the results of the estimation are shown in Figure 5-23.

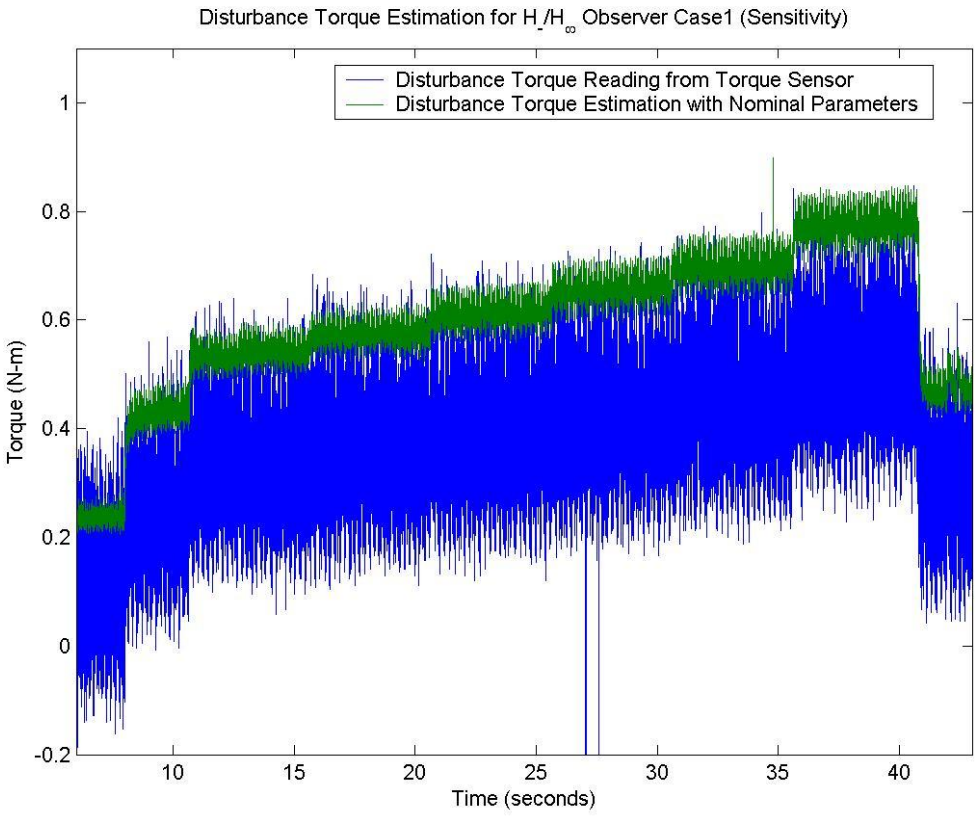

Figure 5-23 Sensitivity Test Results of H_/H∞ Disturbance Torque Estimation Case 1

It can be seen in Figure 5-23 that small changes in the disturbance torque can be detected in the estimation. This is expected since the H_/H∞ observer is designed to maximize the sensitivity of the estimation to the disturbance torque, which is not guaranteed in any other observer design introduced in this thesis. Similar results for case 2 and case 3 are shown in Figure 5-24, 5-25, 5-26 and Figure 5-27, 5-28, 5-29, respectively.

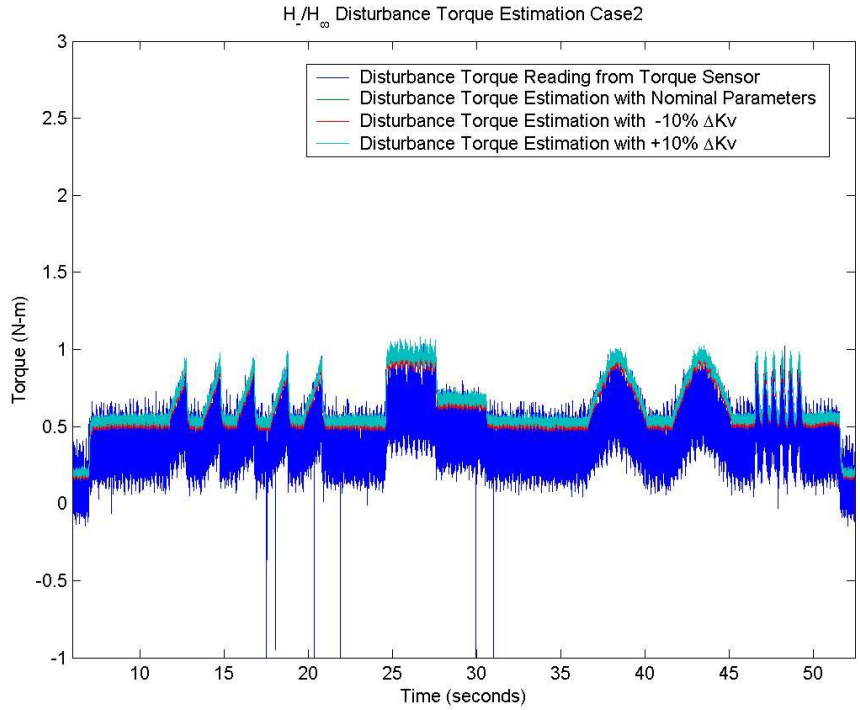

Figure 5-24 Overall Test Results of H_/H∞ Disturbance Torque Estimation Case 2

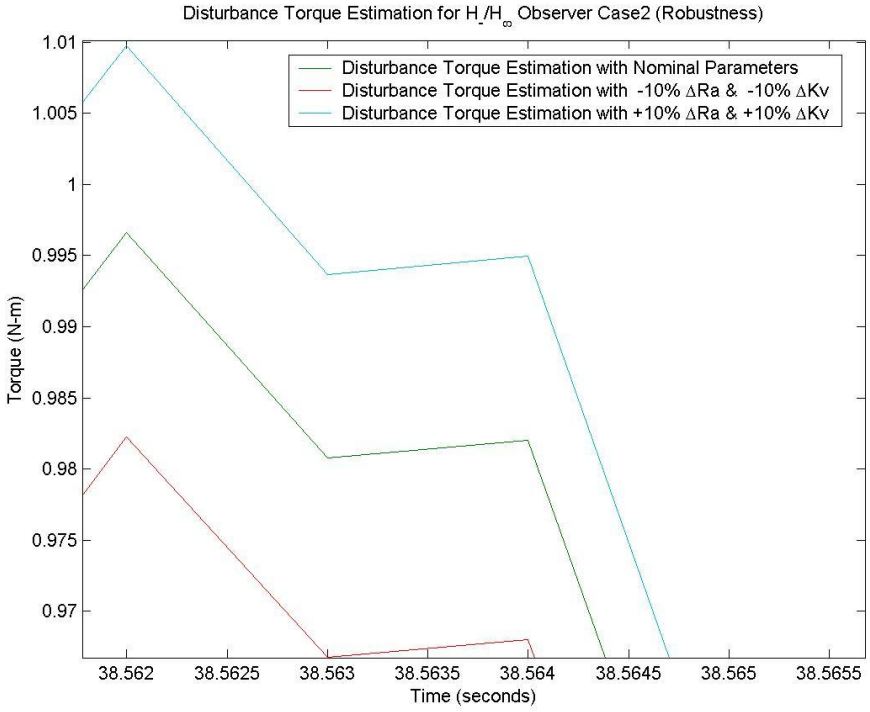

Figure 5-25 Robustness Test Results of H_/H∞ Disturbance Torque Estimation Case 2

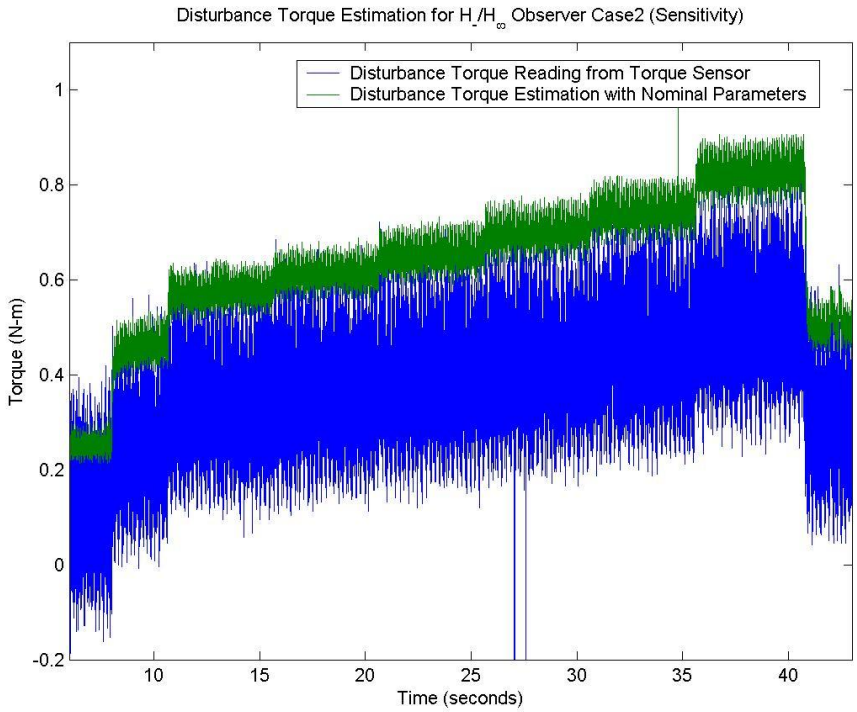

Figure 5-26 Sensitivity Test Results of H_-/H_∞ Disturbance Torque Estimation Case 2

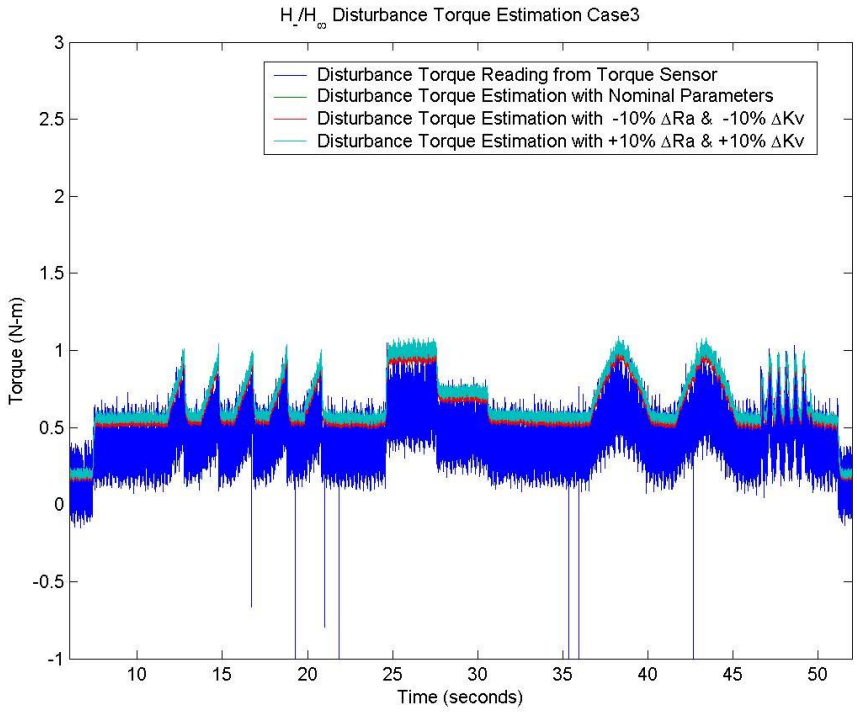

Figure 5-27 Overall Test Results of H_-/H_∞ Disturbance Torque Estimation Case 3

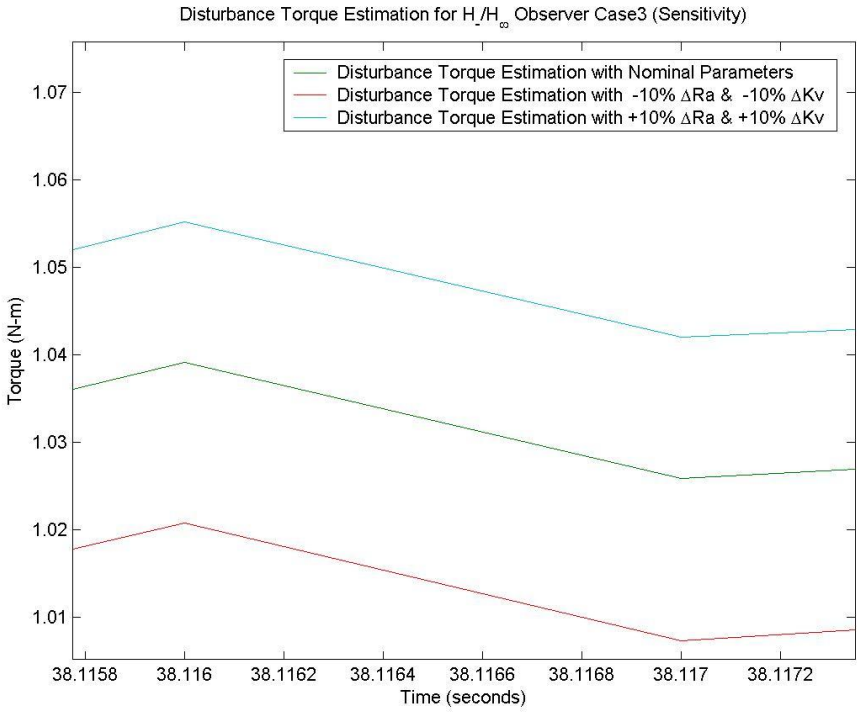

Figure 5-28 Robustness Test Results of H_/H∞ Disturbance Torque Estimation Case 3

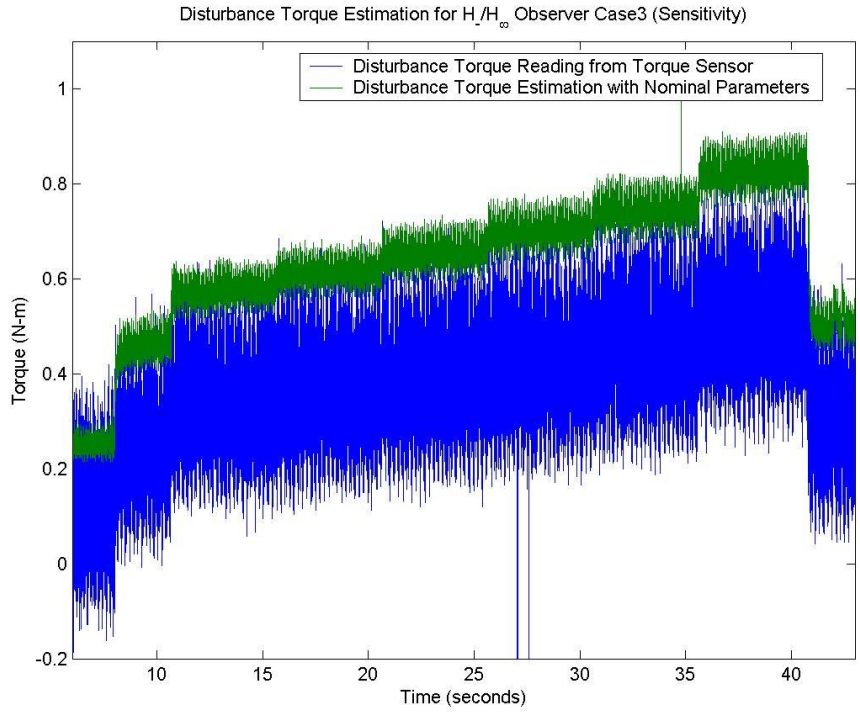

Figure 5-29 Sensitivity Test Results of H_/H∞ Disturbance Torque Estimation Case 3

Based on the test results for all three cases, the estimator design using the H_-/H_∞ observer is verified to deliver an appropriate estimation for both constant and low-frequency disturbance torques. With the finding that the variations between the estimations using nominal parameters and variations of particular parameters are small, the estimator shows robustness to all three cases of model uncertainties. In addition, sensitivity of the estimation to the disturbance torque is also achieved according. By changing the uncertainty attenuation level or the significances of the uncertainties, further improvement of the estimation may be achieved.

CHAPTER 6

CONCLUSION AND FUTURE WORK

6.1 Conclusion

A disturbance torque estimation scheme is developed in this thesis. Due to the advantage that implementation can be done directly and degradation of the estimation can be avoided, the design is conducted in discrete-time. The estimator design consists of a state observer and a disturbance torque calculator.

In order to design an applicable estimator, an appropriate state observer plays a significant role in the overall design. Based on the specific conditions of the applied system, different state observers are discussed and then utilized to deliver a state estimation for use in the disturbance torque calculator. In detail, a Luenberger observer is designed based on a nominal plant model and thus not a desirable choice for application in a real physical system. A Kalman observer is constructed to minimize the effect of undesirable white noises. In the case of a system without accurate modeling, an H_∞ observer is developed to maintain the system's robustness to some model uncertainties. With the finding that a system may be subjected to both white noises and model uncertainties, the performance and robustness requirements can be satisfied by means of a mixed H_2/ H_∞ observer. In addition to rejecting or suppressing some factors, there may

exist some factor that is to be emphasized. In this case, an H_/ H_∞ observer design is carried out to maximize the sensitivity to the disturbance torque while constraining the sensitivity to model uncertainties.

Since a state observer only generates the state estimations and their derivates, a calculator that relates the state estimations to the disturbance torque is required. The disturbance torque calculator is designed using discretization of the system model of a DC motor. Furthermore, an alternative representation of the calculator that relates the torque with the estimation error is also proposed.

The estimator design is tested using a hardware-in-the-loop (HIL) testbench, which provides an environment that reflects the real physical world. In the testbench, a PMDC used as a test motor is attached to a DC dyno motor that provides different types of load disturbance torques. A current shunt resistor is used to measure the armature current of the test motor and an in-line torque sensor is used to validate the estimation results.

Due to the fact that each observer incorporated in the estimator design has its own algorithm and performance criteria, all of the estimator designs are tested in different ways in order to verify that they achieve their desired requirements. For example, all of the estimator designs are tested using a disturbance torque signal which consists of constant and low-frequency signals since this is the basic requirement of the estimator. Then noise tests, robustness tests, and sensitivity tests are performed depending on the specific observer used in the estimator design.

6.2 Future Work

Several state observers contain multiple design parameters. These design parameters have an impact on the performance and the stability of the observer. For each observer with design parameters, some assumptions are made according to the design specifications. However, a wide range for the selection of these parameters results in the need for tuning. Instead of tuning all the parameters by trial and error, some improvements to the observer design may lead to more systematic determination of these parameters.

The results of the disturbance torque estimation can be utilized for control applications. Considering a current-control based DC drive, the estimated disturbance torque can be directly compensated to generate a new reference signal. With the knowledge of this quantity, the controller can achieve better performance. Furthermore, speed control that is not affected by external disturbances can also be realized by means of a dual loop structure.

REFERENCES

[1] Giuseppe S. Buja, Robert Menis, Maria Ines Valla, "Disturbance Torque Estimation in a Sensor-less DC Drive", *IEEE Transactions on Industrial Electronics,* Vol. 42, No. 4, August 1995.

[2] Dan Simon, Kalman Filtering, *Embedded Systems Programming*, vol. 14, No. 6, pp. 72-79, June 2001.

[3] J.Corres, P.Gil, "Instantaneous speed and disturbance torque observer using nonlinearity cancellation of shaft encoder", *Power Electronics Specialists Conference, pesc 02, 2002 IEEE 33rd Annual*, Vol. 2, pp. 540-545

[4] Kemin Zhou, *Essentials of Robust Control*, Prentice Hall, Upper Saddle River, New Jersey, USA, 1988.

[5] William S.Levine, *The Control Handbook*, CRC Press, Boca Raton, Florida, USA, 1999.

[6] Chun-Chih Wang, Masayoshi Tomizuka, "Design of Robustly Stable Disturbance Observers Based on Closed Loop Consideration Using H_∞ Optimization and its Applications to Motion Control Systems", *Proceedings of the 2004 American Control Conference*, 2004, pp. 3764-3769.

[7] Kiyotsugu Takaba, Tohru Katayama, "On the Discrete-Time H_∞ filter via Game Theoretic Approach", *IEEE International Conference on Systems Engineering,* pp. 261-265, September 1992.

[8] Oh-Kyu Kwon, Carlos E.de Souza, Hee-Seob Ryu, "Robust H_∞ FIR Filter for Discrete-Time

Uncertain Systems ", *Proceedings of the 35th on Decision and Control*, Vol. 4, pp. 4819-4824, Kobe, Japan, December, 1996

[9] Xiang Chen, Kemin Zhou, "Multiobjective H_2/ H_∞ Control Design", *SIAM Journal on Control and Optimization*, vol. 40(2), 2001, pp. 628-660.

[10] Ali Tahmasebi, Xiang Chen, "Discrete-Time H_∞ Gaussian Filter", *Proceedingsof the 17th World Congress The International Federation of Automatic Control*, Seoul, Korea, July 6-11, 2008.

[11] Ali Tahmasebi, Xiang Chen, "Discrete-Time Multi-Objective H_2/H_∞ Control", *49th IEEE Conference on Decision and Control*, Atlanta, GA, USA, December 15-17, 2010

[12] Ali Tahmasebi, Xiang Chen, "Discrete-Time H_∞ Gaussian Control", *Proceedings of the 46th IEEE Conference on Decision and Control*, New Orleans, LA, USA, December 12-14, 2007

[13] Nike Liu, Kemin Zhou, "Optimal Solutions to Multi-Objective Robust Fault Detection Problems", *Proceedings of the 46th IEEE Conference on Decision and Control*, pp. 981-988, 2007.

[14] Nike Liu, Kemin Zhou, "Optimal Robust Fault Detection for Linear Discrete Time Systems", *Proceedings of the 46th IEEE Conference on Decision and Control*, pp. 989-994, 2007.

[15] M. Hou, R. J. Patton, "An LMI approach to H_/ H_∞ fault detection observers", *Proceedings of UKACC Inte. Conf. on Control*, 1966, pp. 305-310.

[16] P. M. Frank, X. Ding, "Survey of Robust Residual Generation and Evaluation Methods in Observer-based Fault Detection Systems", J*ournal of Process Control*, 1997, vol. 7, No. 6, pp. 403-424.

[17] Katsuhiko Ogata, *Discrete-Time Control Systems*, Prentice Hall, Upper Saddle River, New Jersey, USA, 1995.

[18] David G. Luenberger, "An Introduction to Observers", *IEEE Transactions on Automatic Control*, vol. AC-16, No. 6, pp. 596-602, 1971.

[19] David G. Luenberger, "Observing the State of a Linear System", *IEEE Transactions on Military Electronics*, vol. MIL-8, pp. 74-80, 1964.

[20] Dan Simon, *Optimal State Estimation*, John Wiley & Sons, Hoboken, New Jersey, USA, 2006.

[21] DC Motor Control. Embedded Systems: DC Motor Control <http://robotics.ee.uwa.edu.au/courses/embedded/tutorials/tutorials/tutorial_6/Tutorial_6.htm> March 18, 2012.

[22] Products: Datasheet DC Motors Without Gear Assembly. "GPA 12V 400W." < http://www.boschmotorsandcontrols.co.uk/elektromotoren/produkt/0130302003/index.htm> 12 April 2012.

[23] Products: DC Motors: CDP3440-V24: Baldor Electrical Company. "Specifications: CDP3440-V24."<http://www.baldor.com/products/specs.asp?1=1&catalog=CDP3440-V24&prod

uct=DC+Motors&family=General+Purpose%7Cvw_DCMotors_GeneralPurpose> 12 April 2012.

[24] Roboteq, Inc. “Roboteq AX3500 Dual Channel High Power Digital Motor Controller User’s Manual.” USA, Roboteq, Inc., 2003-2007.

[25] Roboteq, Inc. “Roboteq AX1500 Dual Channel Digital Motor Controller User’s Manual.” USA, Roboteq, Inc., 2003-2007.

[26] Current Shunt Resistors. “RC Electronics: Current Shunt Resistors” <http://www.rc-electronics-usa.com/current-shunt.html> April 10, 2012

[27] Sensor Developments Inc. “Rotating Torque Sensor with Digital Telemetry Model: 01424 Operators Manual.” USA. June 17, 2010.

[28] User’s Guide. “User’s Guide for TQ513 Rotary Torque Sensor”<http://www.omega.com/manuals/manualpdf/M4898.pdf> April 13, 2012

[29] Opal-RT Technologies Inc. “RT-Lab v6.0 User’s Manual.” Canada. Opal-RT Technologies Inc., 2002.

VITA AUCTORIS

NAME: Huijie Qian

PLACE OF BIRTH: Shanghai, P. R. China

EDUCATION: University of Windsor, Windsor, Ontario, Canada

2010-2012, M.A.Sc

Shanghai Jiaotong University, Shanghai, P. R. China

2006-2010, B.Eng